# Hierarchical screening for Li-based solid electrolytes using fast, interpretable machine-learned potentials

Stephen R. Xie[1], Shreyas J. Honrao[1], John W. Lawson[2]

[1] KBR Inc, NASA Ames Research Center

[2] NASA Ames Research Center, Moffett Field, CA, USA

- Pipeline for high-throughput ionic conductivity predictions
- Validating bond valence methods for screening solid-state electrolytes
- Automatic fitting of ultra-fast, interpretable machine-learning force fields

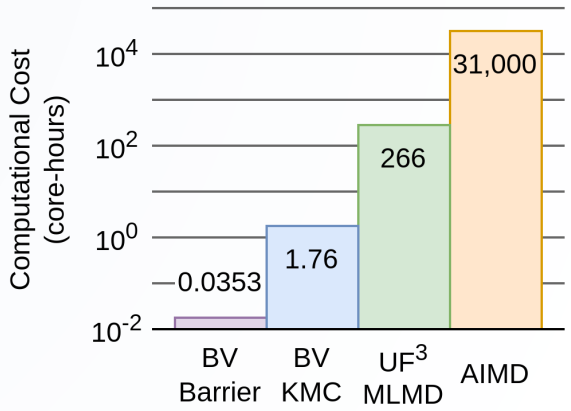

# Background

- All Solid-State Batteries with Li anode
  - Safety
  - Energy density
  - Charging rate
- Solid-state Electrolyte
  - High ionic conductivity
  - Low electronic conductivity
  - Good electrochemical stability
  - Abundance, low-cost, manufacturability, etc.

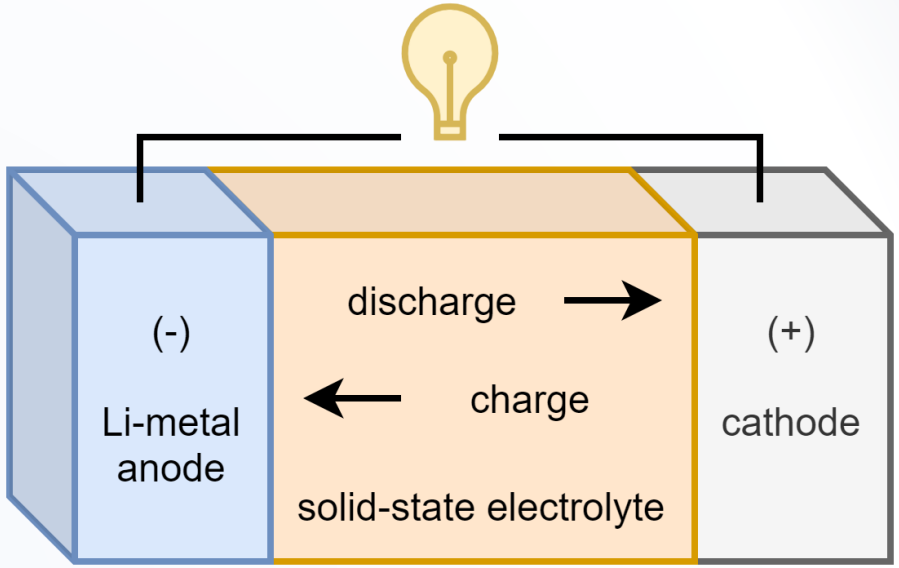


nasa.gov

Honrao, S.J., Yang, X., Radhakrishnan, B. *et al.* Discovery of novel Li SSE and anode coatings using interpretable machine learning and high-throughput multi-property screening. *Sci Rep* **11**, 16484 (2021). https://doi.org/10.1038/s41598-021-94275-5

# Computational Screening

- Honrao et al. 2021
  - Generated database of battery-related material properties
  - Screening
    - Thermodynamic stability
    - Electrochemical stability
    - Band gap
  - Trained interpretable machine learning models to predict bond valence (BV) migration barriers, oxidation and reduction potentials
- Migration barrier is a proxy for ionic conductivity
- Goal: construct framework to efficiently compute ionic conductivity for screening

| Type | Property | Symbol | Units |
|---|---|---|---|
| Stability | Energy above convex hull | $E_{hull}$ | eV/atom |
| | Oxidation potential | $V_{oxi}$ | V |
| | Reduction potential | $V_{red}$ | V |
| Device | Band gap | $E_g$ | eV |
| | Shear modulus | G | GPa |
| Transport | Vacancy formation energy | $E_V$ | eV |
| | Migration barrier | $E_M$ | eV |
| | Ionic conductivity | $\sigma_{300K}$ | mS/cm |

Honrao, S.J., Yang, X., Radhakrishnan, B. *et al.* Discovery of novel Li SSE and anode coatings using interpretable machine learning and high-throughput multi-property screening. *Sci Rep* **11**, 16484 (2021).

# Ionic Conductivity

- Mean squared displacement (MSD)
  - For Li, should grow linearly with time in ionic conductors
  - MSD = $\left\langle \left[ \overrightarrow{r(t)} - \overrightarrow{r(0)} \right]^2 \right\rangle$
- Diffusion coefficient
  - $D = \frac{1}{2d} \log_{t \to \infty} \left\langle \left[ \overrightarrow{r(t)} - \overrightarrow{r(0)} \right]^2 \right\rangle$
  - For 3D system (d=3), fit from one-sixth of slope of MSD vs. time
- Ionic Conductivity: $\sigma = \frac{\eta q^2}{k_B T} D$

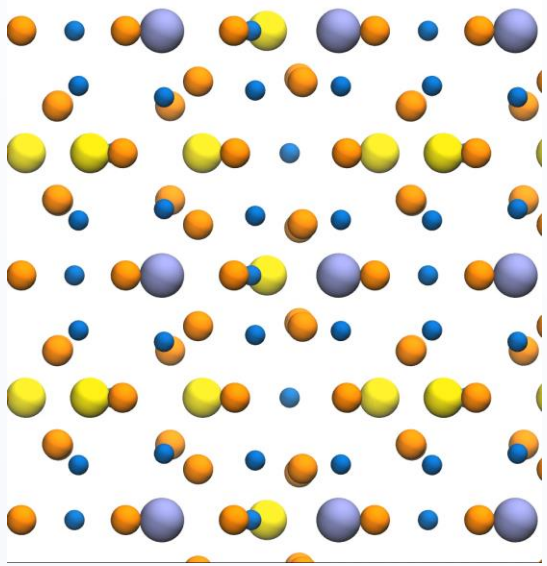

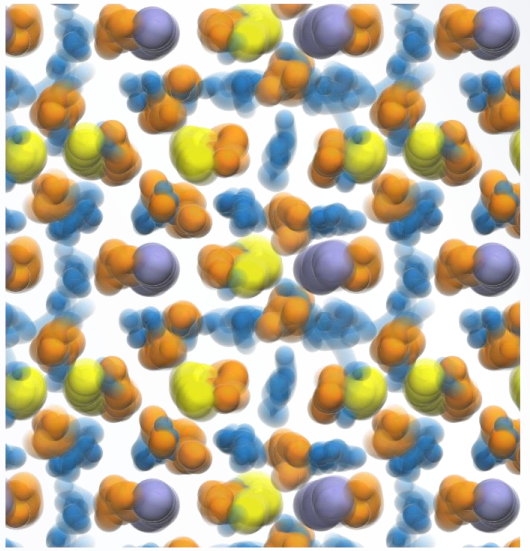

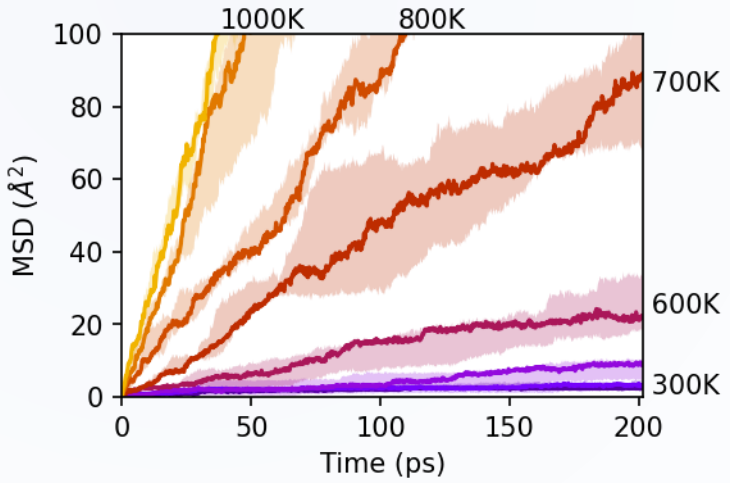


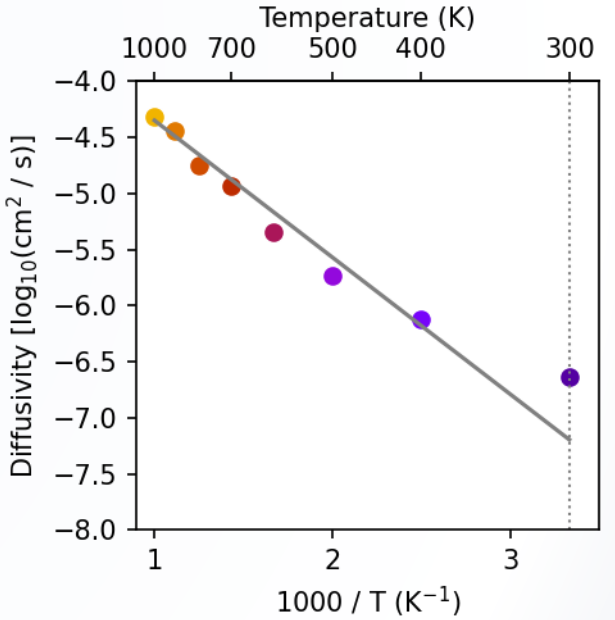

$Li_{10}GeP_2S_{12}$

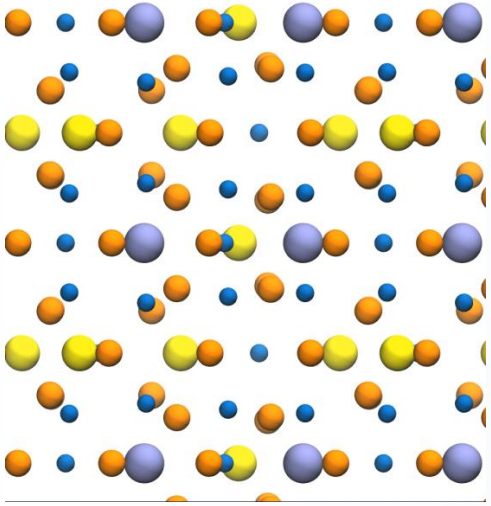

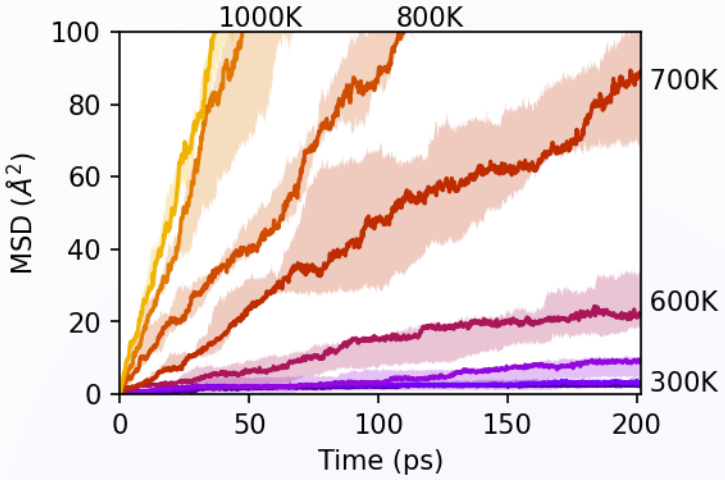


$Li_4P_2O_7$

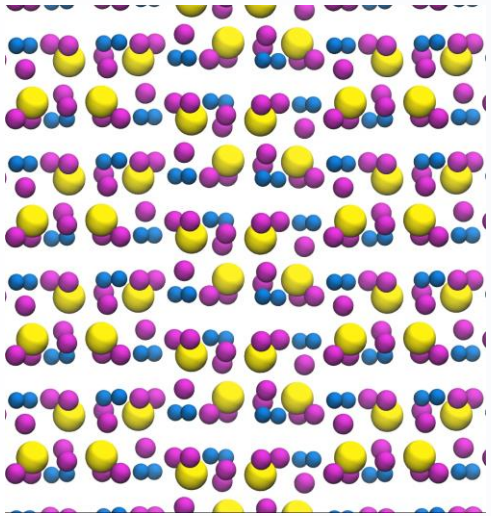

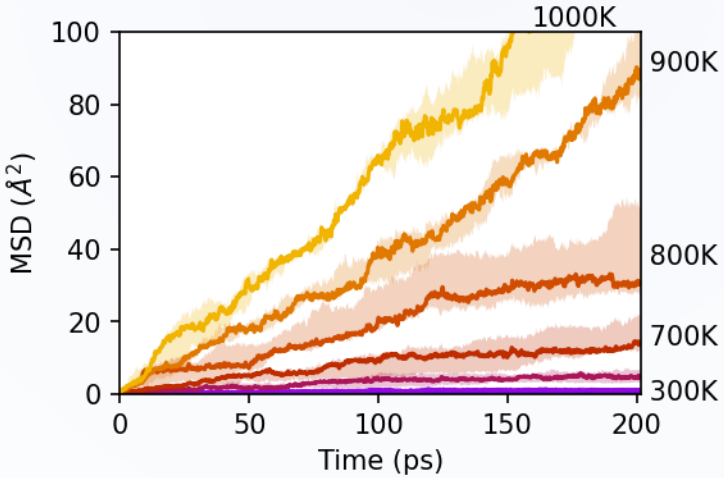


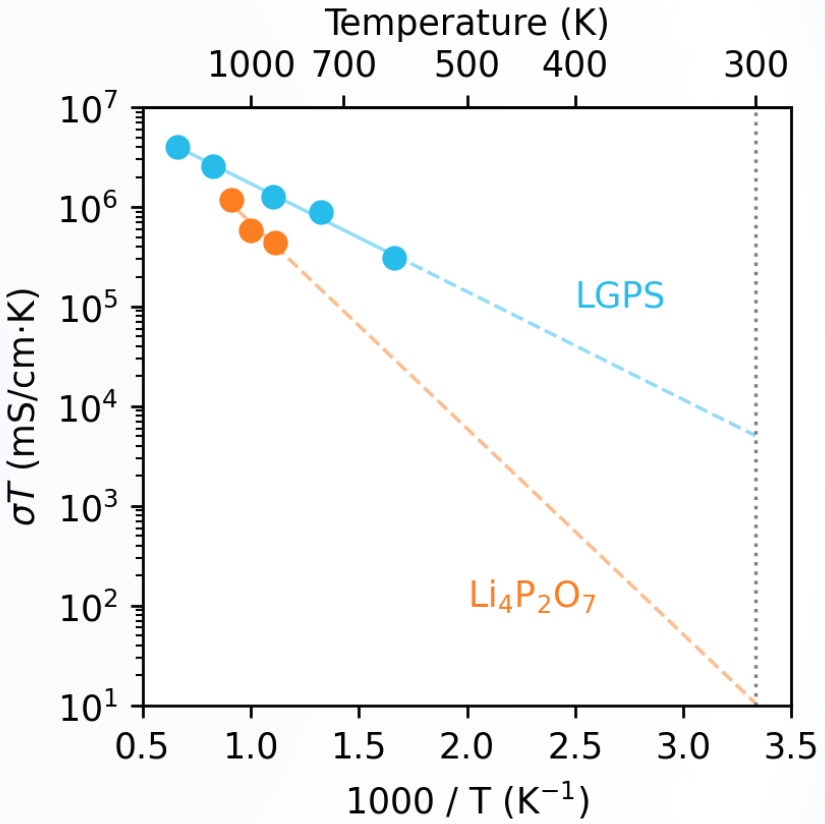

# High-throughput searches

| | | Number of candidates | | | Number of Transport calculations | | |
|---|---|---|---|---|---|---|---|
| | Data source | Initial | Before transport | Final | Pathway Analysis | MD | First Principles |
| Honrao et al. 2021 | Materials Project | 15466 | 15466 | ~250 | 15446 | - | - |
| Sendek et al. 2017 | Materials Project | 12831 | 317 | 21 | - | - | - |
| Sendek et al. 2019 | Materials Project | 12831 | 317 | 12 | - | - | 41 (AIMD) |
| Muy et al. 2019 | Materials Project | ~14,000 | ~14,000 | 18 | - | - | ~1000 Phonon Band centers |
| Kahle et al. 2020 | ICSD and COD | 7472 | 1016 | 47 | - | 916 | 132 (AIMD) |
| Wang et al. 2020 | Materials Project | 1545 | 234 | 5 | - | 19 | 19 (AIMD at 1000 K) |
| Wang et al. 2021 | Materials Project | 1545 | 274 | 25 | - | 36 | 274 (AIMD at 1000 K) |
| Xiao et al. 2019 | ICSD | 104082 | 184 | 6 | - | - | 7 NEB barriers |
| Xiao et al. 2021 | ICSD | 6242 | 53 | 7 | - | - | 12 (AIMD at 1000K), 10 (AIMD) |
| Jun et al. 2022 | Materials Project | 8572 | 122 | 22 | - | - | 56 (AIMD at 1000K), 22 (AIMD) |
| Sundberg et al. 2022 | Materials Project | 9747 | 3174 | 12 | - | - | 6797 IDDP, 299 NEB barriers |
| Zhao et al. 2022 | Materials Project | 16205 | 87 | 2 | 87 | - | 9 (AIMD) |

# Validation set for ionic conductivity

- Existing ab initio molecular dynamics (AIMD) studies
- Diversity in composition, structure, and ionic conductivity

## AIMD

- PBE-DFT
- Large supercell
- Gamma-point only
- 100-500 picoseconds for diffusivity convergence
- Repeat for multiple temperatures to fit Arrhenius relationship

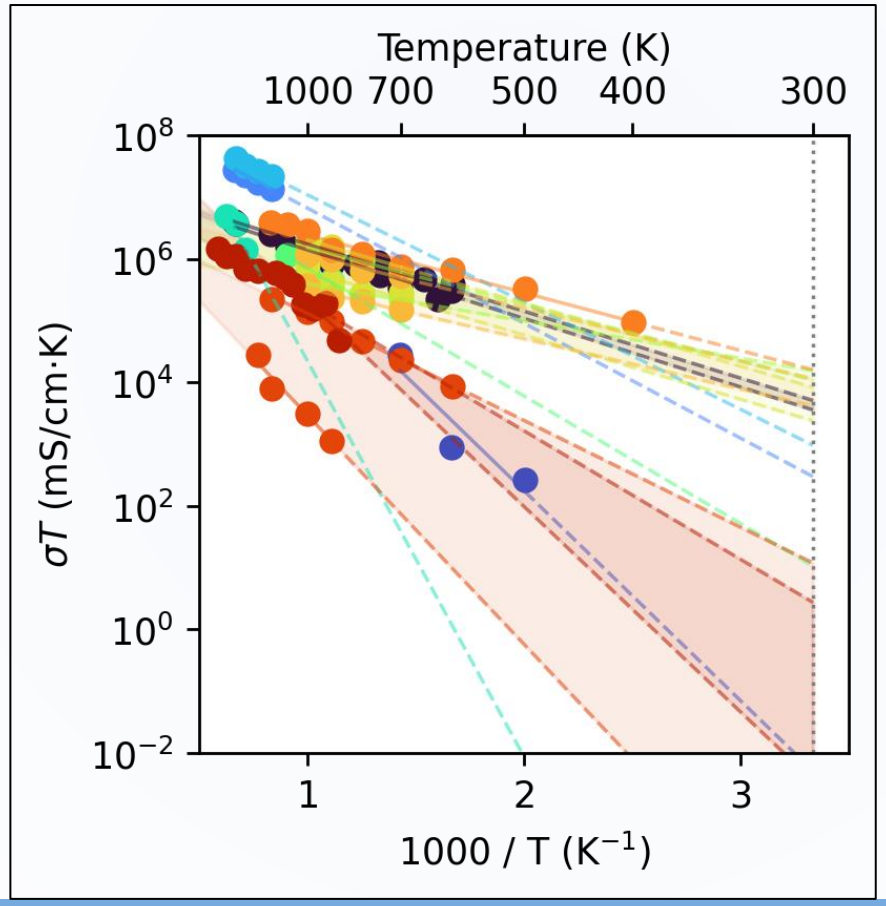


| Formula | MPID | Category |
|---|---|---|
| $Li_7P_3S_{11}$ | mp-641703 | thio-LISICON |
| $Li_{10}GeP_2S_{12}$ | mp-696128 | thio-LISICON |
| $Li_6PS_5Cl$ | mp-985592 | Argyrodite |
| $Li_6PS_5Br$ | mp-985591 | Argyrodite |
| $Li_6PS_5I$ | mp-985582 | Argyrodite |
| $Li_3AlF_6$ | mp-15254 | Group IIIA Halide |
| $Li_3GaF_6$ | mp-15558 | Group IIIA Halide |
| $LiZr_2P_3O_{12}$ | mp-10499 | Li-NASICON |
| $LiTi_2P_3O_{12}$ | mp-18640 | Li-NASICON |
| $Li_4P_2O_7$ | mp-554577 | Oxide |
| $Li_2SO_4$ | mp-4556 | Oxide |
| $Li_4GeO_4$ | mp-4558 | Oxide |

# Methods – Speed and accuracy

- AIMD are accurate
- Bond valence methods are fast
  - Migration barriers from pathway analyses (BVPA) are correlated to ionic conductivity
  - Ionic conductivity requires Kinetic Monte Carlo (KMC)
  - softBV
- Machine-learned force fields
  - Require first-principles data for fitting
  - Machine-learned molecular dynamics (MLMD)
  - Ultra-Fast Force Fields ($UF^3$)

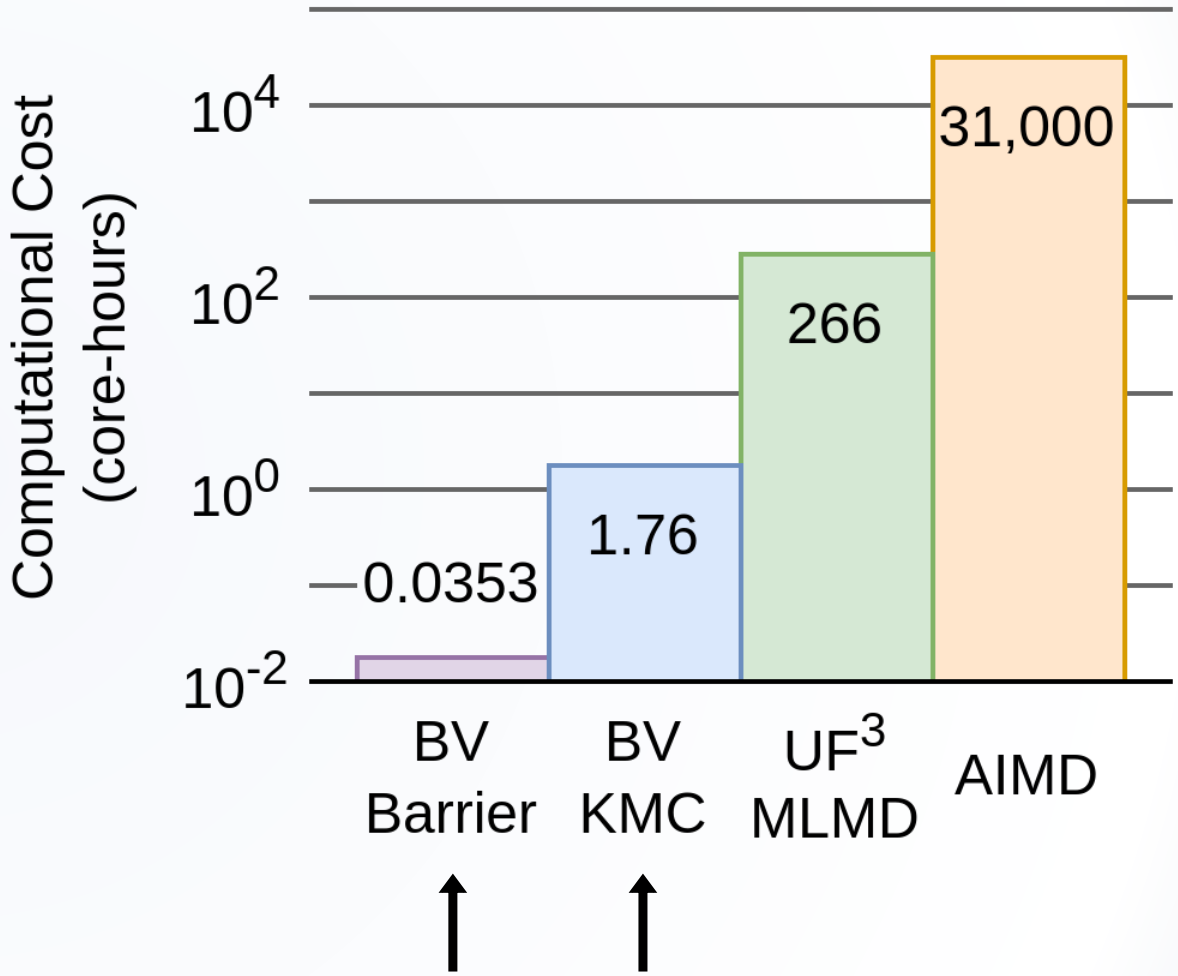

# Bond valence methods with softBV

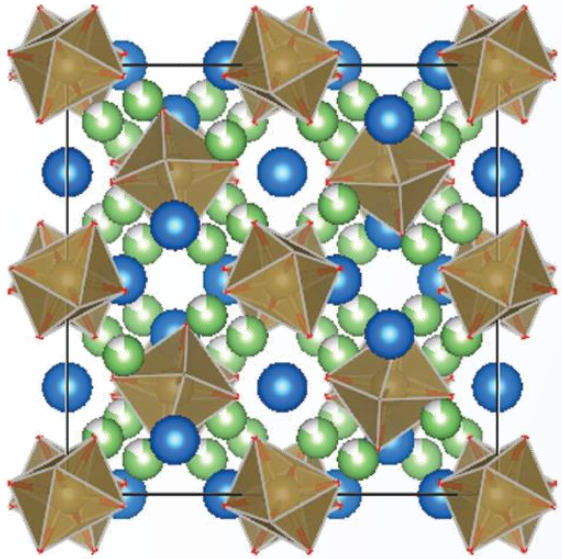

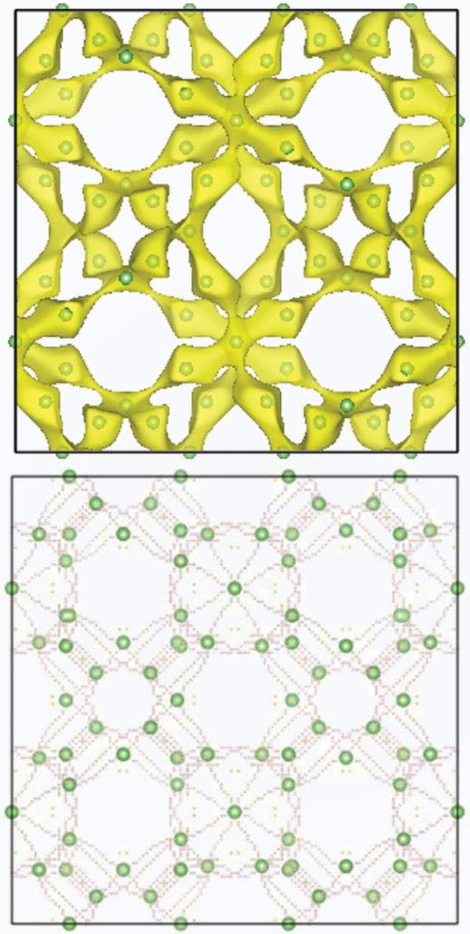

$$E_{\text{bond}} = D_0\left[\exp\left(\frac{R_{\min} - R}{b}\right) - 1\right]^2 - D_0$$

$$E_{\text{Coul}} = \frac{q_1 q_2}{R}\operatorname{erfc}\left[\frac{R}{f(r_1 + r_2)}\right]$$

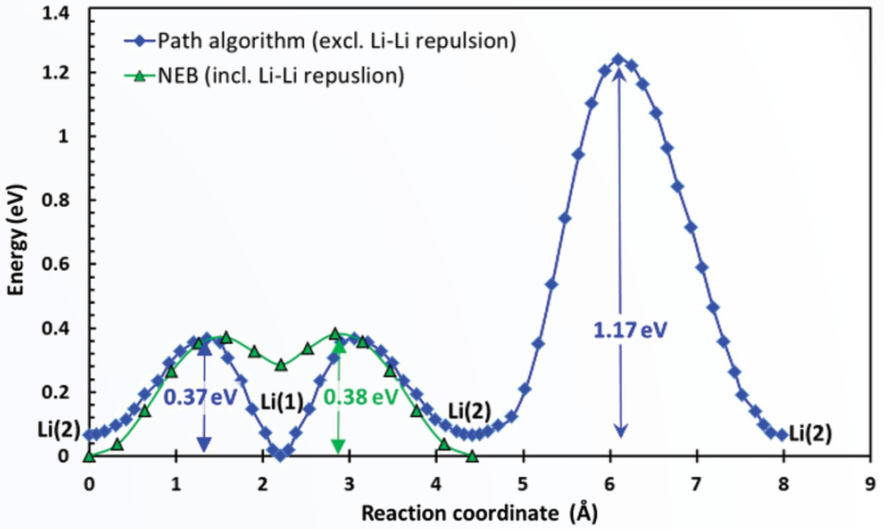


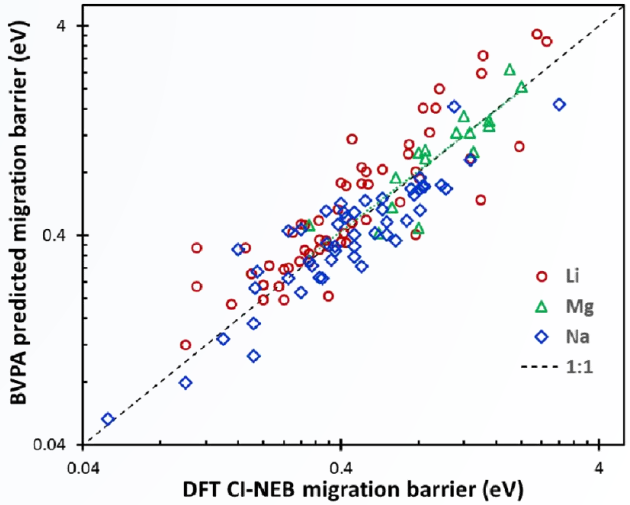


Excellent agreement with migration barriers from climbing-image nudged elastic band calculations (DFT CI-NEB)

# Bond valence methods with softBV

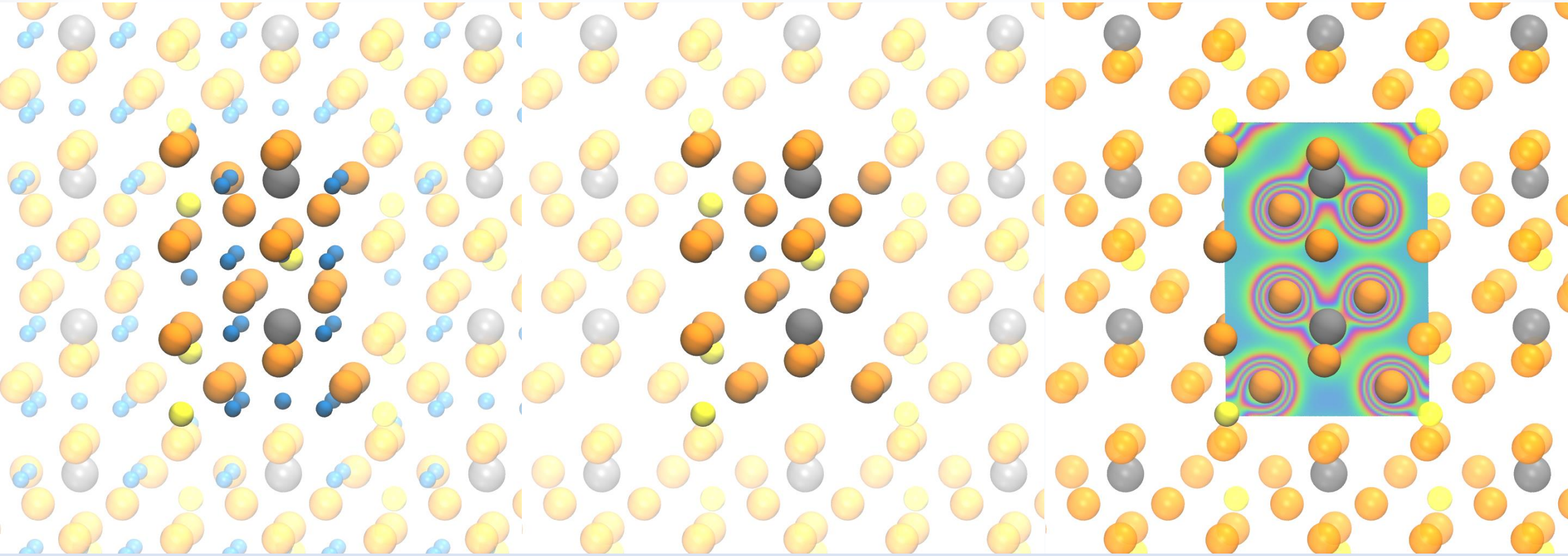

- Energy landscape of single Li atom sampled uniformly with bond valence force field
- Non-Li atoms are immobile, Li-Li interaction ignored

# Bond valence methods with softBV

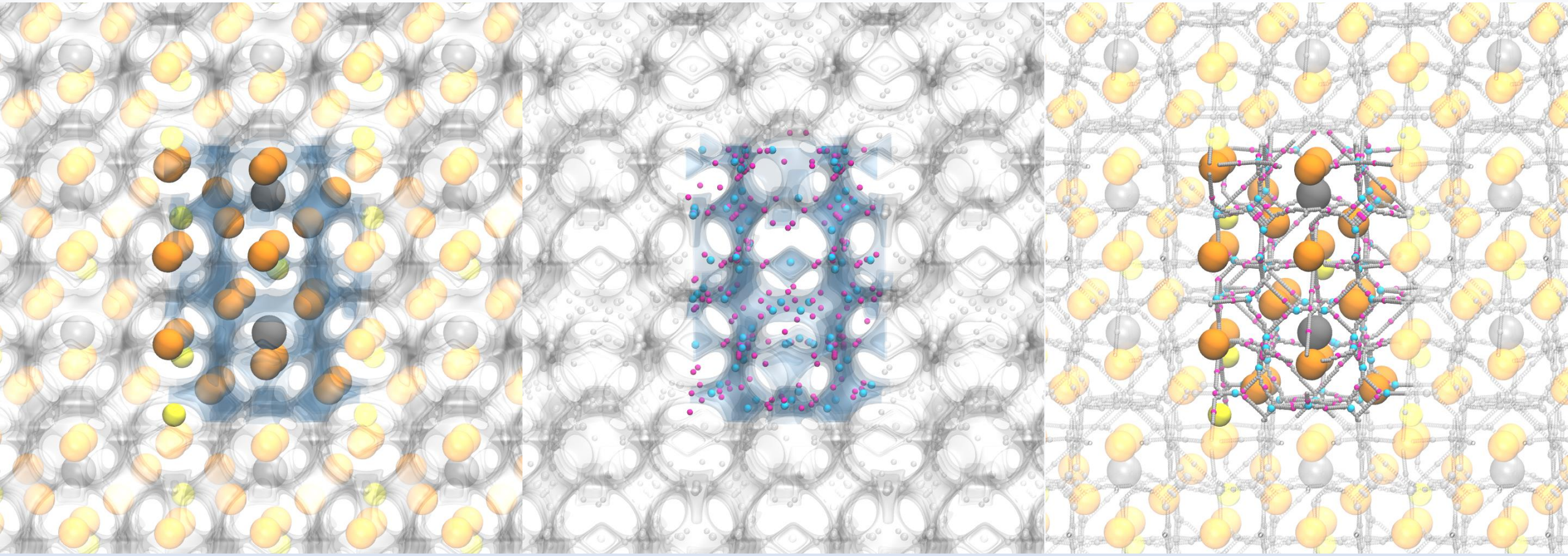

- Low-energy regions reveal percolation pathways for Li
- Pathways connect saddle points and local minima in energy landscape

# Bond valence methods with softBV

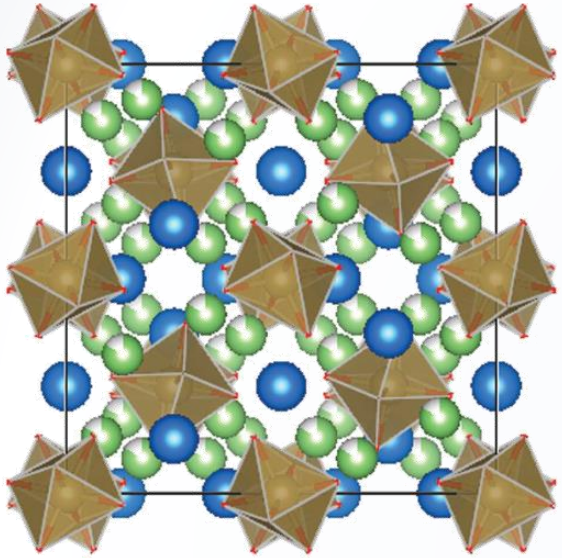

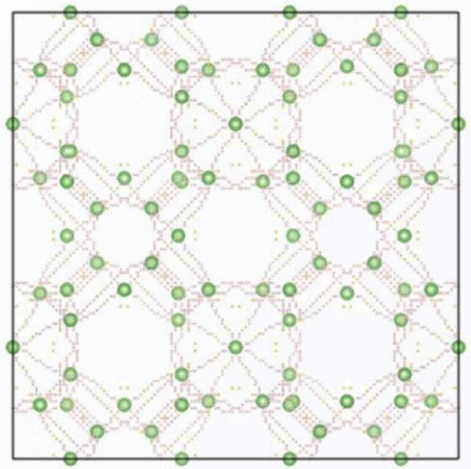

$$p = \omega \exp\left(-\frac{E_m + \Delta E}{k_B T}\right)$$

$$D = \frac{1}{6}\log_{t\to\infty}\left\langle\left[\overrightarrow{r(t)} - \overrightarrow{r(0)}\right]^2\right\rangle$$

$$\sigma = \frac{\eta q^2}{k_B T} D$$

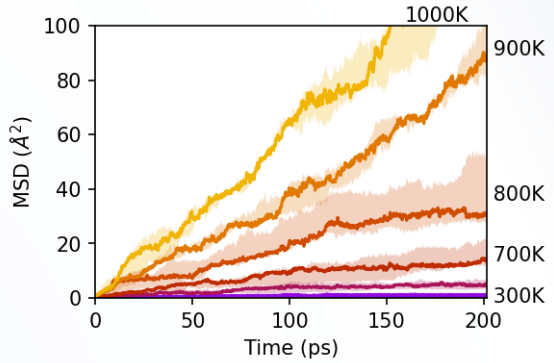


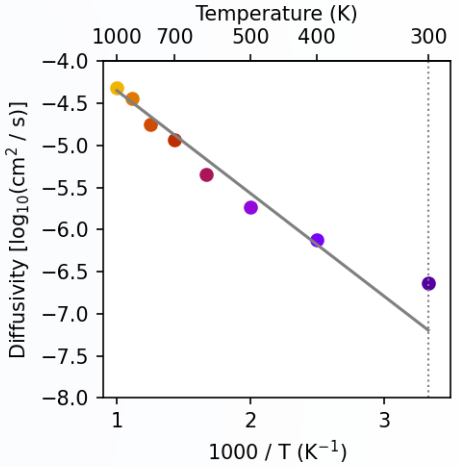


Kinetic Monte Carlo (KMC)

1) Construct graph where vertices are interstitial or equilibrium Li sites
2) Generate supergraph such that lattice parameters are $\geq 25$ Å
3) Distribute Li (set occupancy to 1.0) to sites with lowest energies
4) Equilibrate and run the KMC, adjusting migration barriers based on repulsion from instantaneous arrangement of Li on nearby sites
5) Fit diffusion constant from MSD
6) Compute ionic conductivity from diffusion constant

- $p$: transition rate for hops to vacant, adjacent sites
- $\omega$: attempt frequency
- $E_m$: migration barrier
- $\Delta E$: local Li-Li repulsion

H. Chen, L. L. Wong and S. Adams. SoftBV – a software tool for screening the materials genome of inorganic fast ion conductors. Acta Cryst. (2019). B75, 18-33.

# Methods – Speed and accuracy

- AIMD are accurate
- Bond valence methods are fast
  - Migration barriers from pathway analyses (BVPA) are correlated to ionic conductivity
  - Ionic conductivity requires Kinetic Monte Carlo (KMC)
  - softBV
- Machine-learned force fields
  - Require first-principles data for fitting
  - Machine-learned molecular dynamics (MLMD)
  - Ultra-Fast Force Fields ($UF^3$)

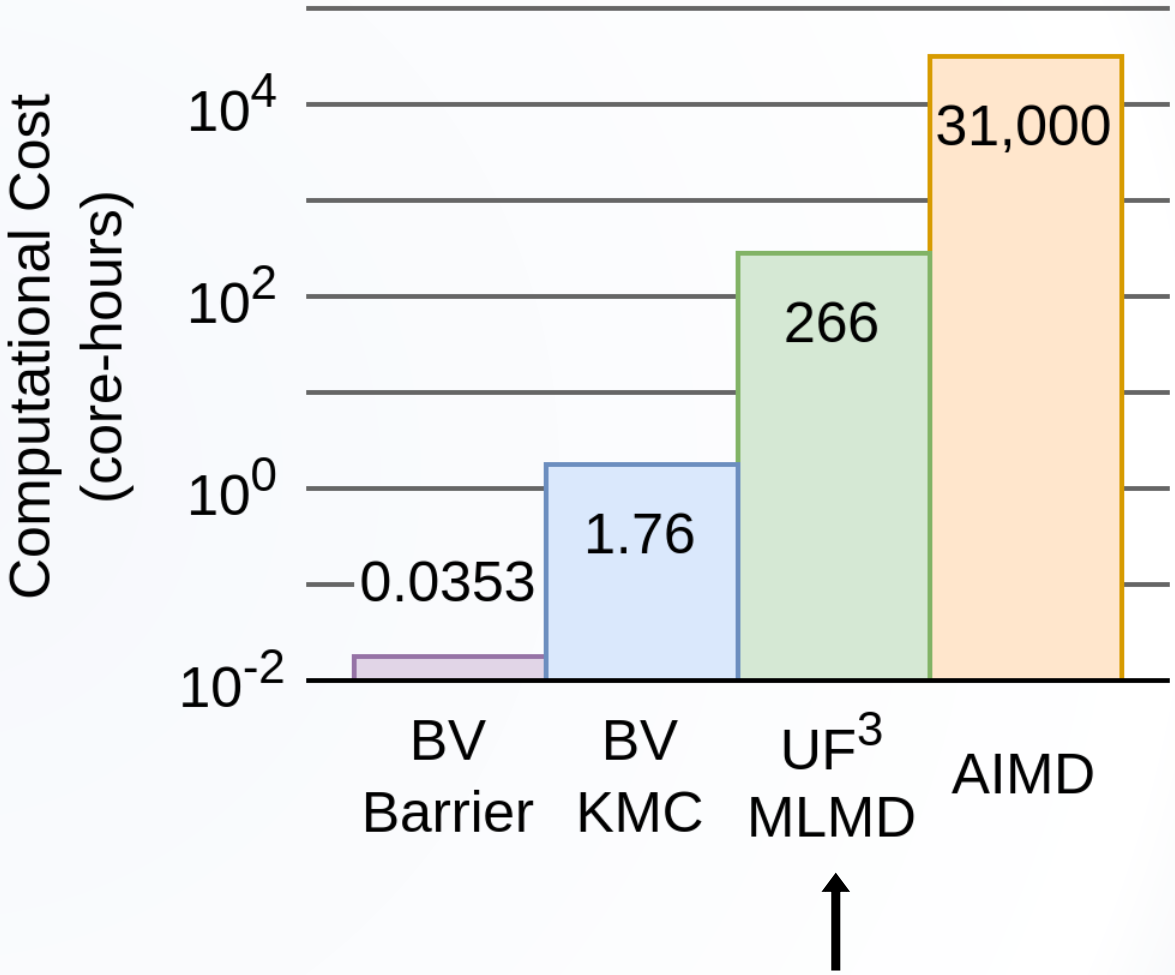

# Ultra-Fast Force Fields ($UF^3$)

- As fast as empirical potentials
- Accurate enough for applications
- Robust
- Interpretable
- Easy to parametrize

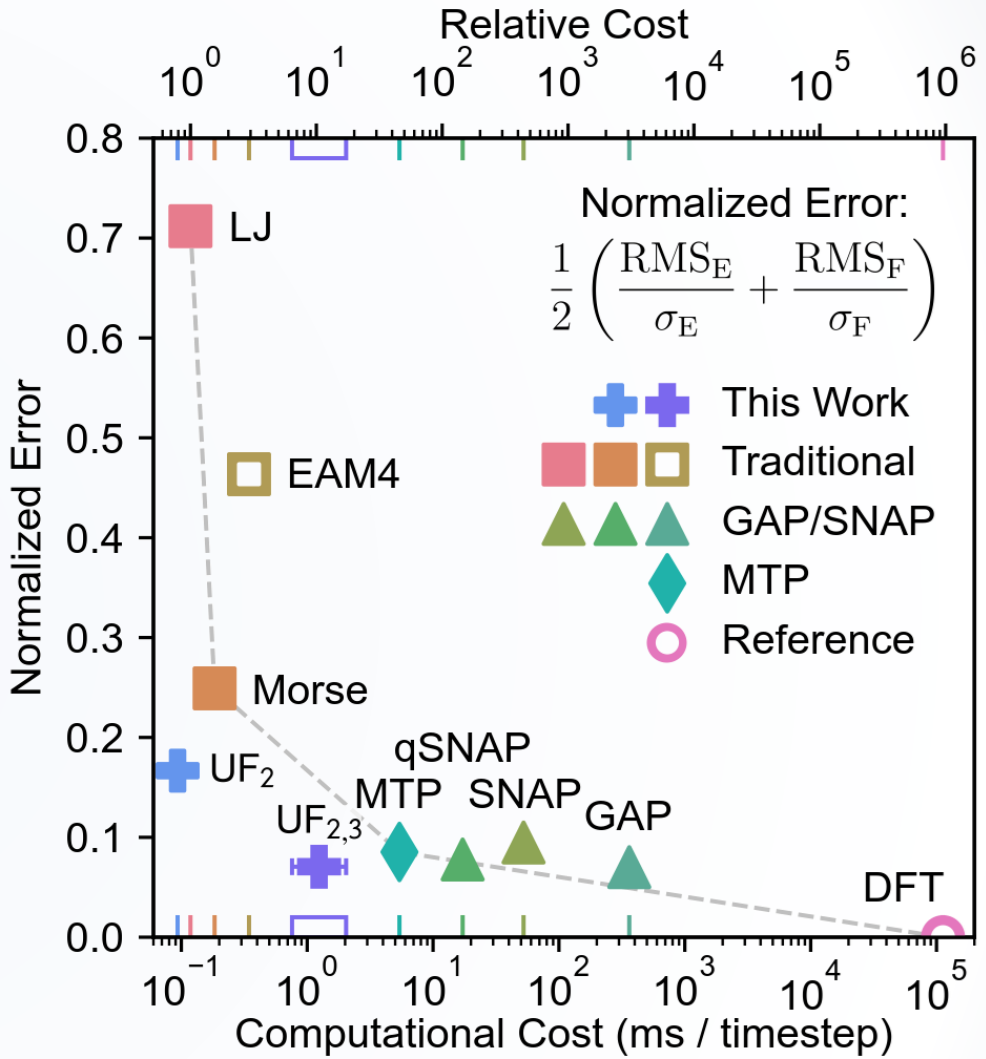


*Tungsten; Szlachta et al., PRB, 2014*

# Ultra-Fast Force Fields (UF$^3$)

- Effective two-and-three body potential
- Cubic B-spline basis set
  - Local support
  - Smooth 1st derivative
  - Continuous 2nd derivative

$$E = \sum_{i<j} V_2(r_{ij}) + \sum_{i<j<k} V_3(r_{ij}, r_{ik}, r_{jk})$$

$$V_2(r_{ij}) = \sum_{n=-2}^{K-1} c_n N_{n,3}(r_{ij}) \qquad r_{ij} = \sqrt{(R_i - R_j)^2}$$

$$V_3(r_{ij}, r_{ik}, r_{jk}) = \sum_{l=-3}^{K_l-1} \sum_{m=-3}^{K_m-1} \sum_{n=-3}^{K_n-1} c_{lmn} \left( N_{l,3}(r_{ij}) N_{m,3}(r_{ik}) N_{n,3}(r_{jk}) \right)$$

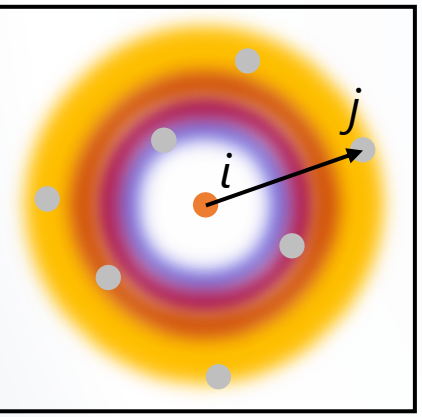


$$N_{n,d+1}(r) = \frac{r - t_n}{t_{n+d} - t_n} N_{n,d}(r) + \frac{t_{n+d+1} - r}{t_{n+d+1} - t_{n+1}} N_{n+1,d}(r) \qquad N_{n,1}(r) = \begin{cases} 1, & r \in [t_n, t_{n+1}] \\ 0, & \text{otherwise} \end{cases}$$

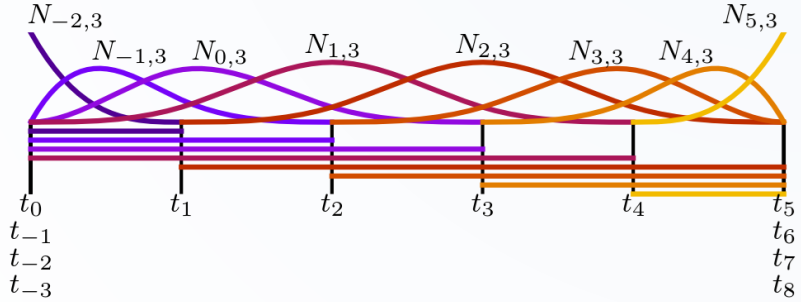


B-splines are defined recursively.
Cubic B-splines have degree d=3.

The UF potential is a sum of cubic B-spline basis functions, weighted by spline coefficients *c*

# Ultra-Fast Force Fields (UF$^3$)

$$E_{2,1} = V_2(r_{12}) + V_2(r_{13}) + V_2(r_{14})$$

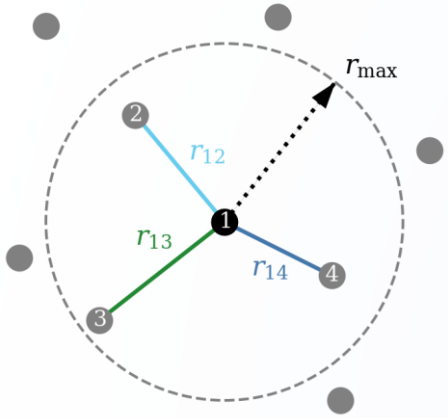


$$V_2(r_{ij}) = \sum_{n=-2}^{K-1} c_n N_{n,3}(r_{ij})$$

- Number of basis functions controls maximum local curvature of the b-spline
- Smooth cutoff(s) by constraining coefficients

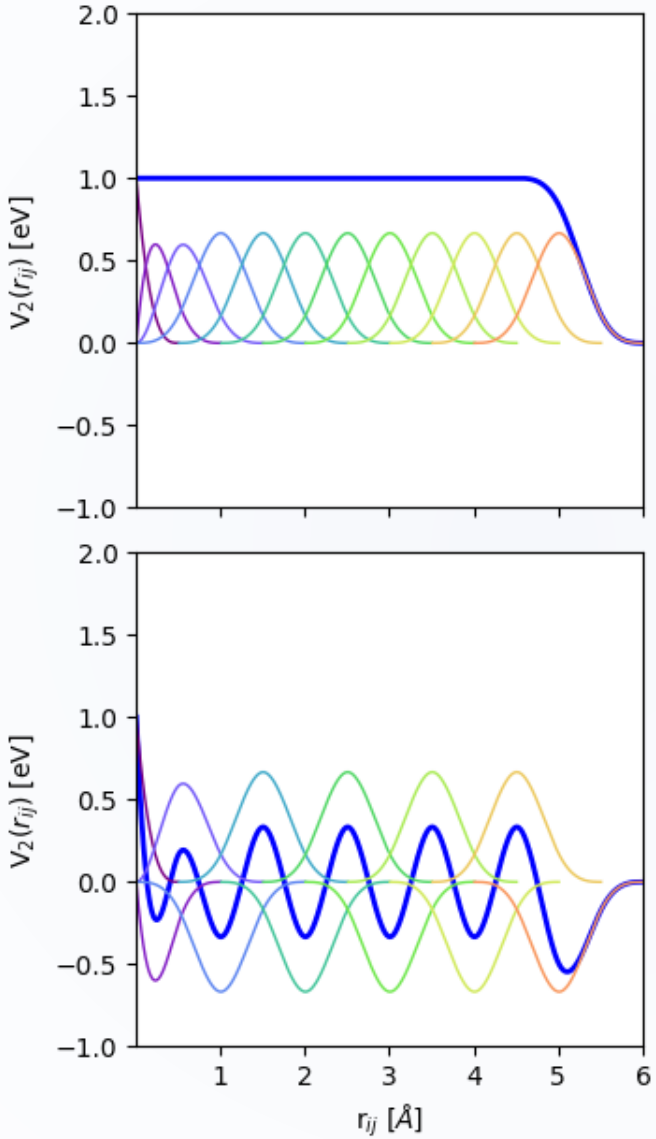


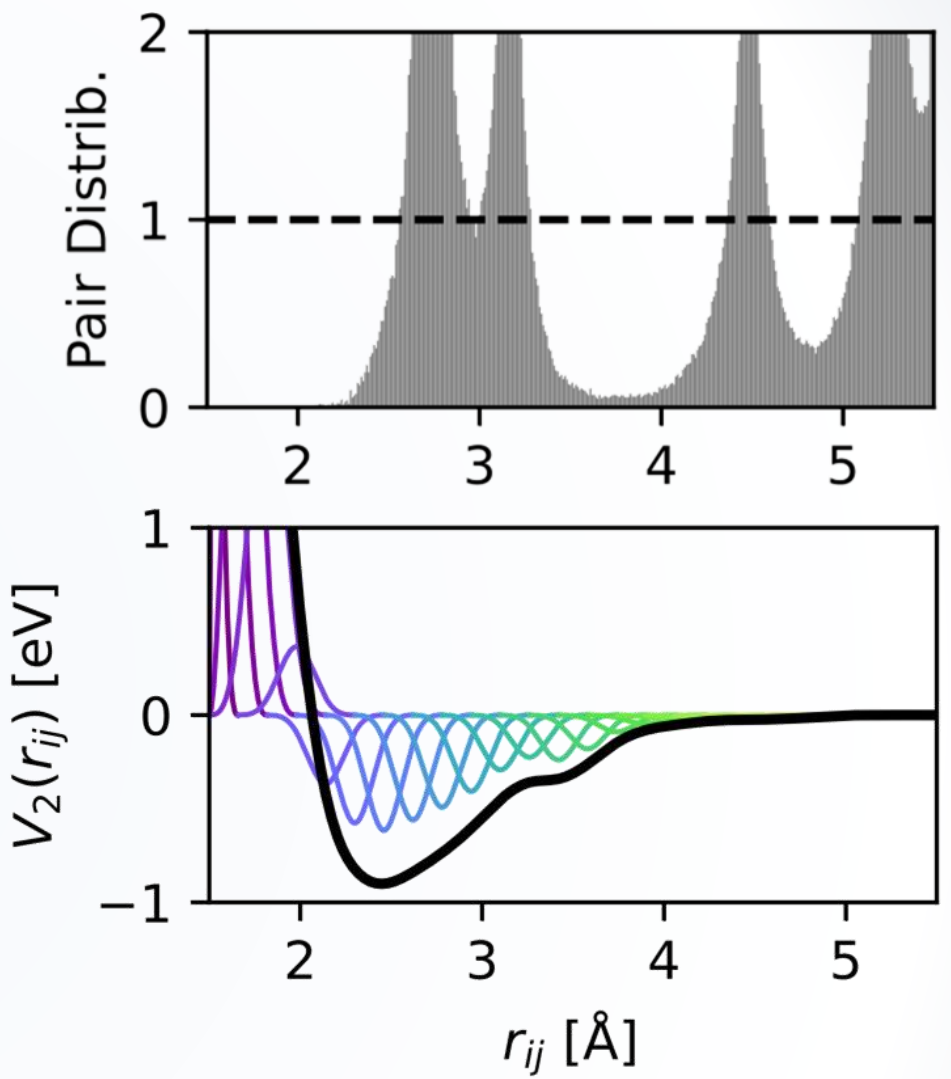


**Tungsten, 2-body**: attractive and repulsive regions; Potential minimum is close to the known nearest-neighbor distance (2.7 Å).

# Ultra-Fast Force Fields (UF$^3$)

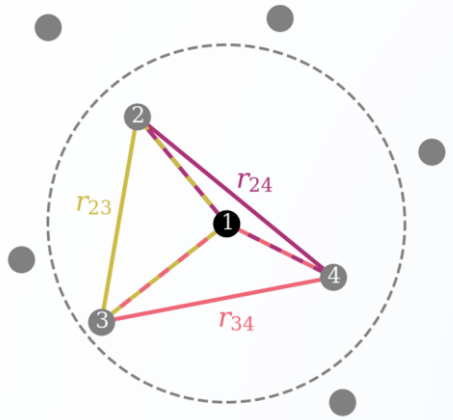


$$E_{3,1} = V_3(r_{12}, r_{13}, r_{23}) + V_3(r_{12}, r_{14}, r_{24}) + V_3(r_{13}, r_{14}, r_{34})$$

$$V_3(r_{ij}, r_{ik}, r_{jk}) = \sum_{l=-3}^{K_l-1} \sum_{m=-3}^{K_m-1} \sum_{n=-3}^{K_n-1} c_{lmn} \left( N_{l,3}(r_{ij}) N_{m,3}(r_{ik}) N_{n,3}(r_{jk}) \right)$$

- 3D tensor-product spline
- Fit simultaneously with two-body term during least-squares optimization
- Visualization
  - Blue: favorable interactions
  - Red: unfavorable interactions

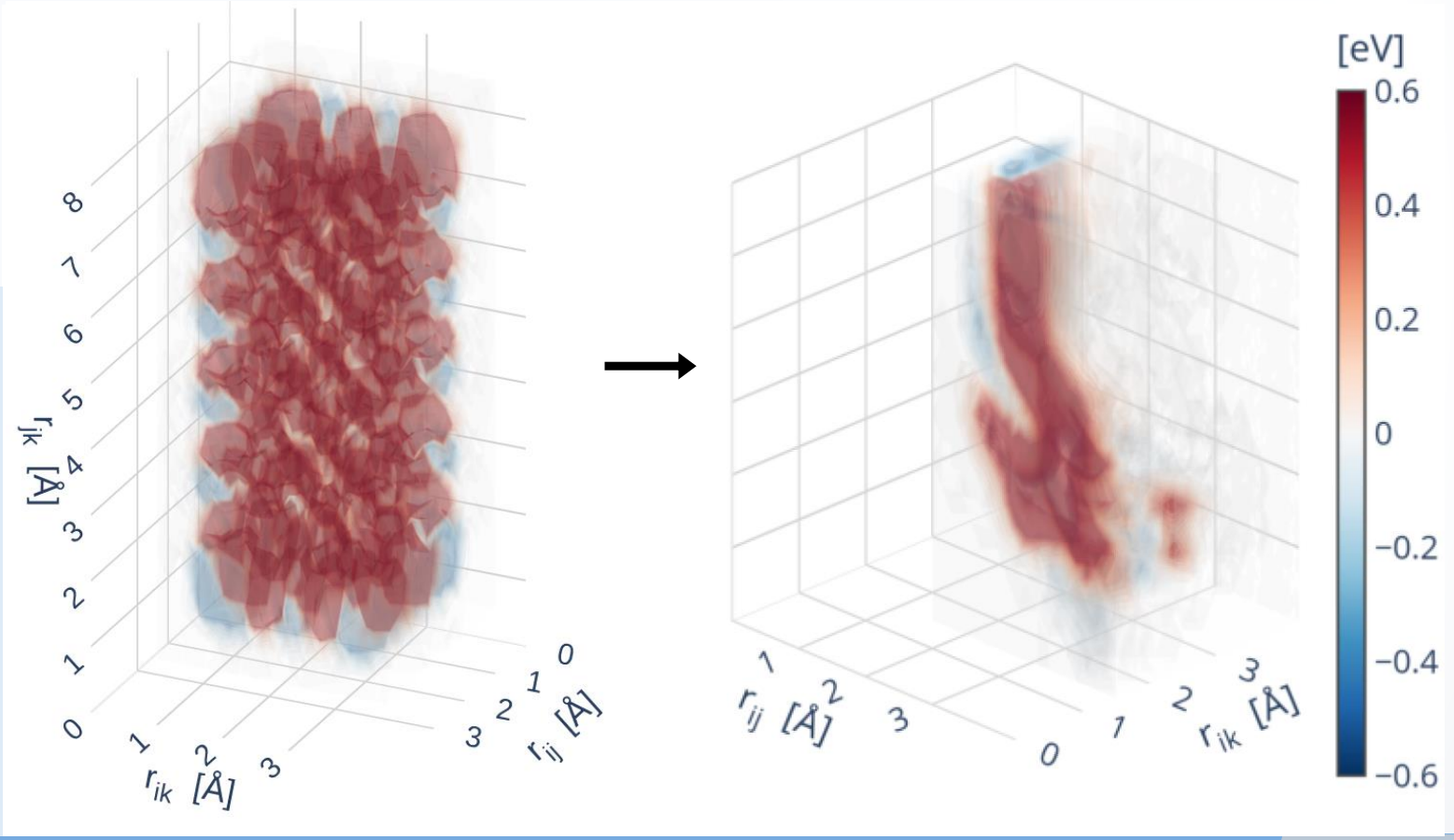

# Ultra-Fast Force Fields (UF$^3$)

$$V_3(r_{ij}, r_{ik}, r_{jk}) = \sum_{l=-3}^{K_l-1} \sum_{m=-3}^{K_m-1} \sum_{n=-3}^{K_n-1} c_{lmn} \left( N_{l,3}(r_{ij}) N_{m,3}(r_{ik}) N_{n,3}(r_{jk}) \right)$$

- Inspect b-spline function for unphysical “holes”
- Three-body term can be visualized with $\theta_{jik}$ instead of $r_{jk}$ for improved interpretability (law of cosines)

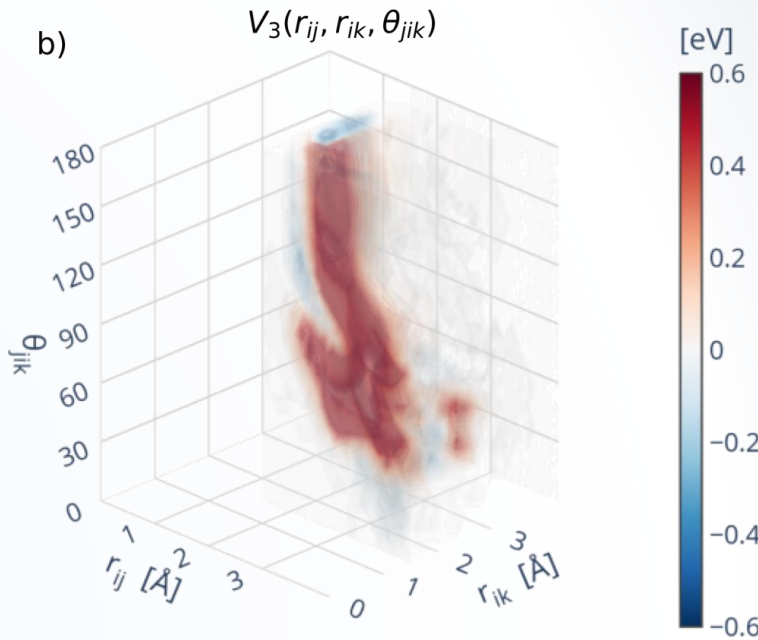


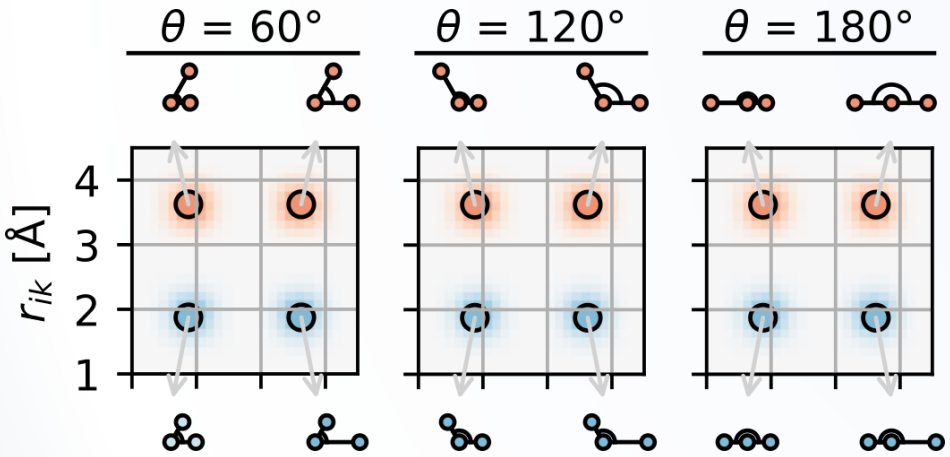


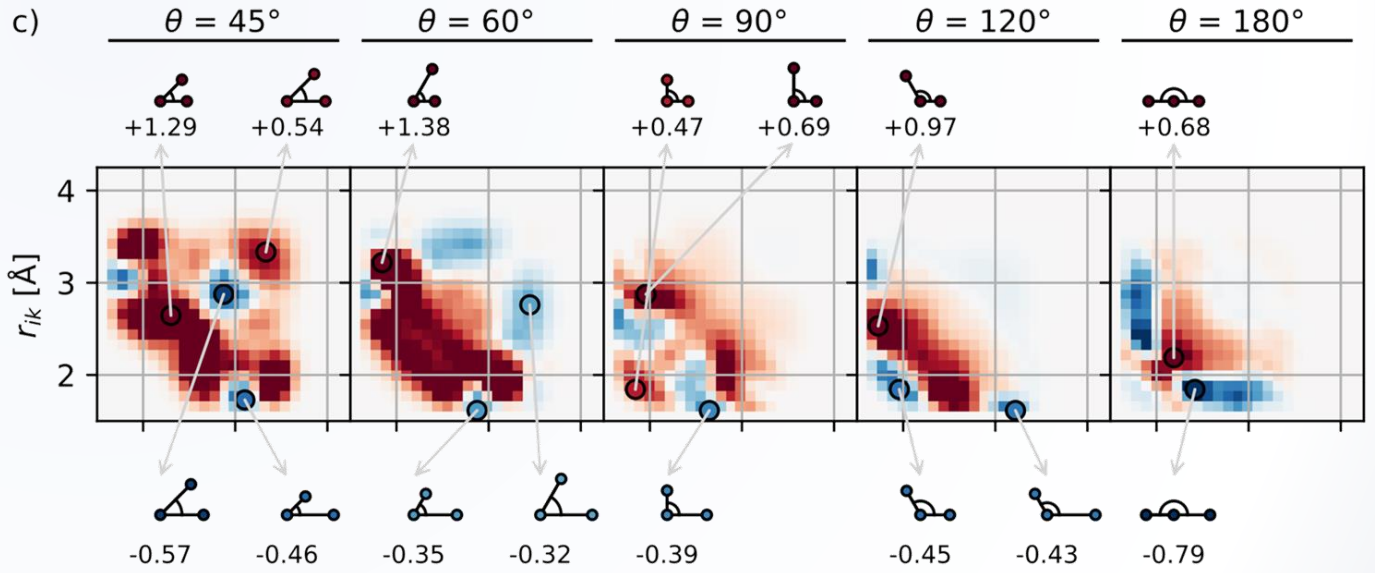

# Ultra-Fast Force Fields (UF$^3$)

- Inputs (X): B-spline structure representation
- Outputs (y)
  - Potential energy from DFT
  - Interatomic forces from DFT
    - Negative gradient of energy
    - [3 x number of atoms] forces per structure
- Hyperparameters
  - Energy-force tradeoff, κ
  - Regularization strength for two-body and three-body coefficients, $\lambda_2$ and $\lambda_3$

$$x_{s,n,AB} = \sum_{i \in A}^{N_s} \sum_{j \in B}^{\infty} N_{n,3}(r_{ij})$$

$$x_{s,lmn,ABC} = \sum_{i \in A}^{N_s} \sum_{j \in B}^{\infty} \sum_{k \in C}^{\infty} N_{n,3}(r_{ij}) N_{l,3}(r_{ik}) N_{m,3}(r_{jk})$$

$$Xc = y \qquad y = \begin{bmatrix} y_1 \\ \vdots \\ y_S \end{bmatrix}$$

$$c = \begin{bmatrix} c_{1,AA} \\ \vdots \\ c_{n,BC} \\ c_{111,AAA} \\ \vdots \\ c_{lmn,CBA} \end{bmatrix}$$

$$X = \begin{bmatrix} x_{1,1,AA} & \cdots & x_{1,n,BC} & x_{1,111,AAA} & \cdots & x_{1,lmn,CBA} \\ \vdots & \ddots & \vdots & \vdots & \ddots & \vdots \\ x_{S,1,AA} & \cdots & x_{S,n,BC} & x_{S,111,AAA} & \cdots & x_{S,lmn,CBA} \end{bmatrix}$$

$$\lambda = \begin{bmatrix} \lambda_2 & & & & & 0 \\ & \ddots & & & & \\ & & \lambda_2 & & & \\ & & & \lambda_3 & & \\ & & & & \ddots & \\ 0 & & & & & \lambda_3 \end{bmatrix}$$

$$c = (X^T X + \lambda I)^{-1} X^T y$$

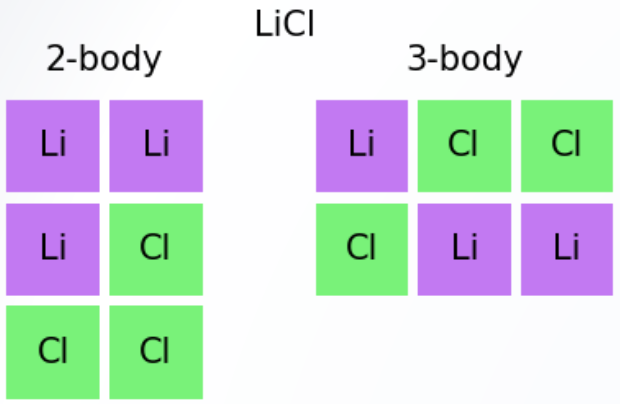


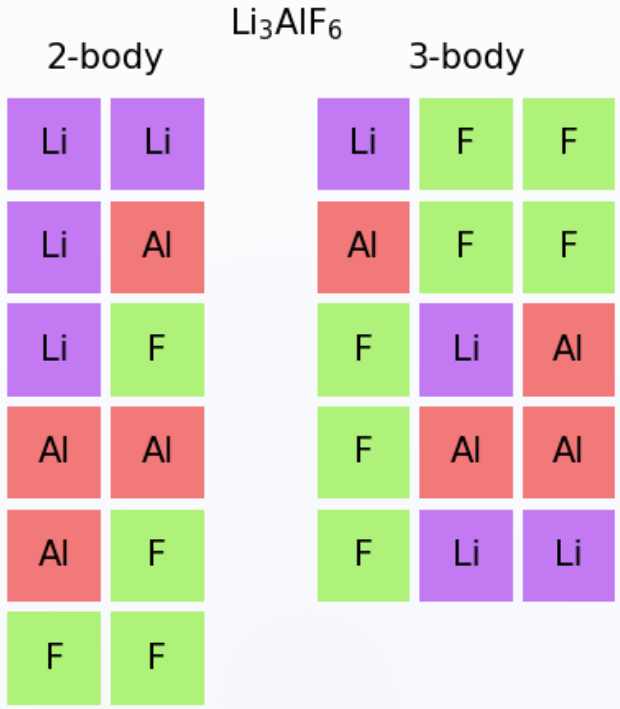


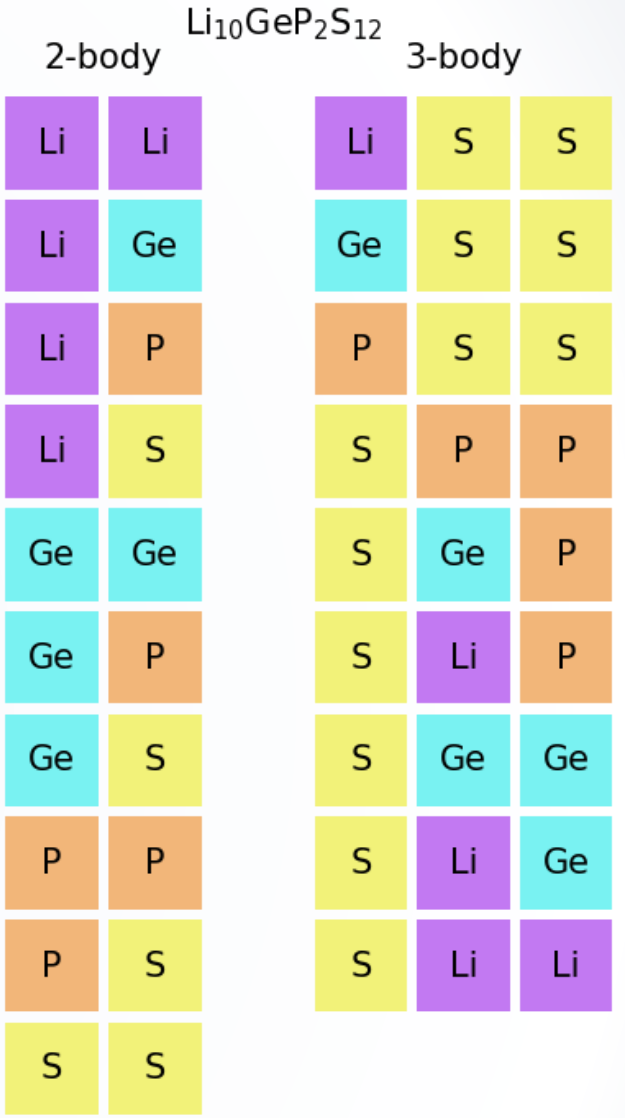


- 2-body:
  25 coeff. / interaction
- 3-body:
  250 coeff. / interaction

- Reduce fitting complexity and improve data efficiency by ignoring subset of chemical interactions
- Disable cation-anion-cation and anion-cation-anion three-body interactions without losing accuracy

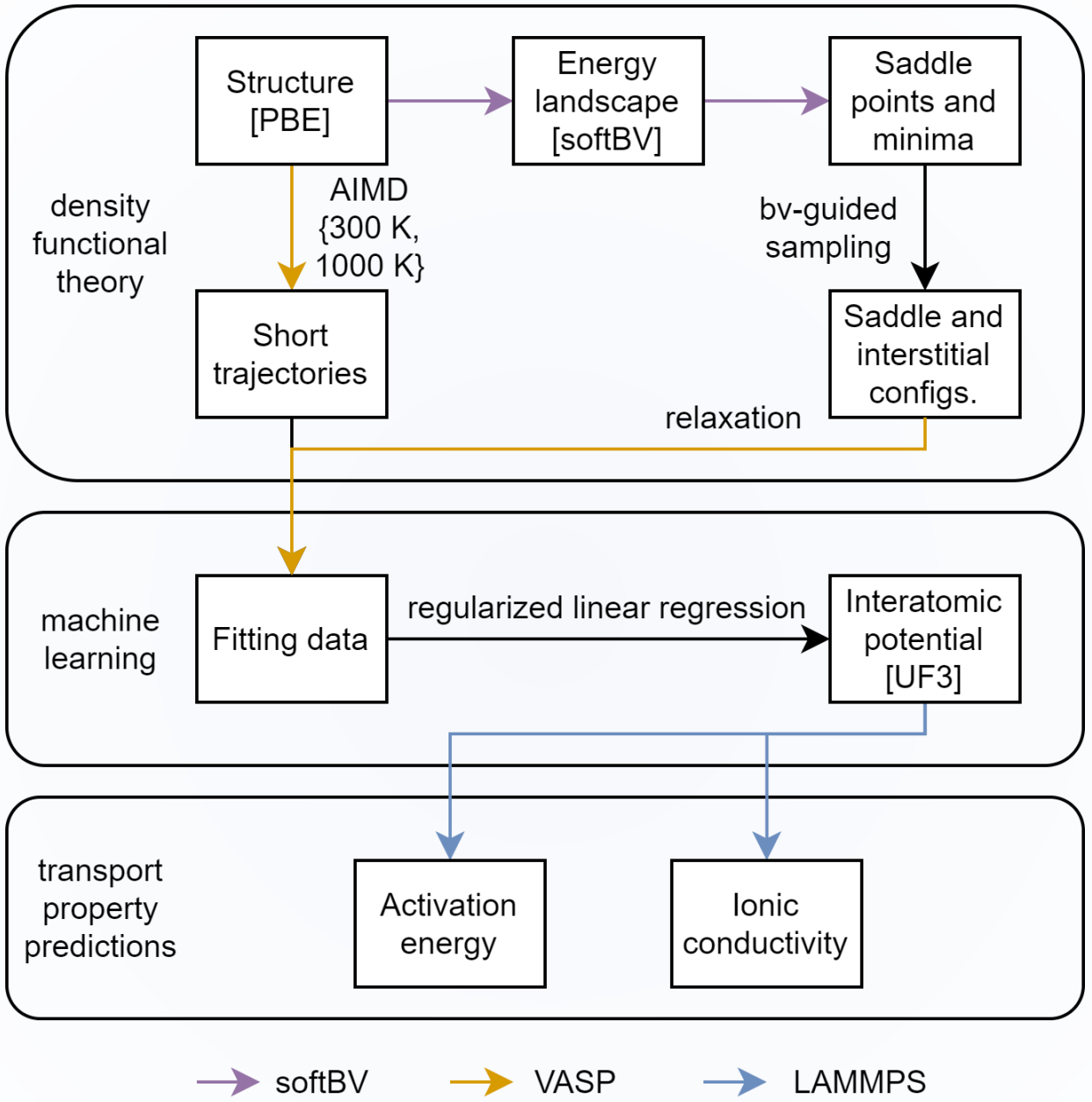
Structure [PBE]
Energy landscape [softBV]
Saddle points and minima
density functional theory
AIMD {300 K, 1000 K}
bv-guided sampling
Short trajectories
Saddle and interstitial configs.
relaxation
machine learning
Fitting data
regularized linear regression
Interatomic potential [UF3]
transport property predictions
Activation energy
Ionic conductivity
softBV
VASP
LAMMPS

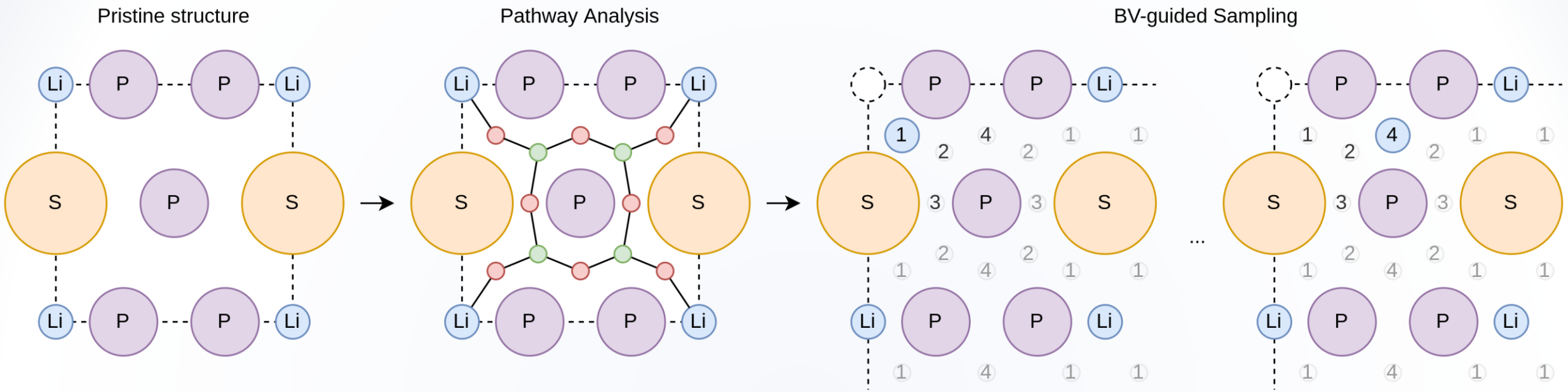


- BV-guided sampling
  - For each saddle point or local minimum in softBV energy landscape (node), identify closest N lithium sites based on BV pathways
  - For each site-node pair, generate a configuration by moving the Lithium from the site to the node (creating a Frenkel defect)
- Lithium vacancy configurations

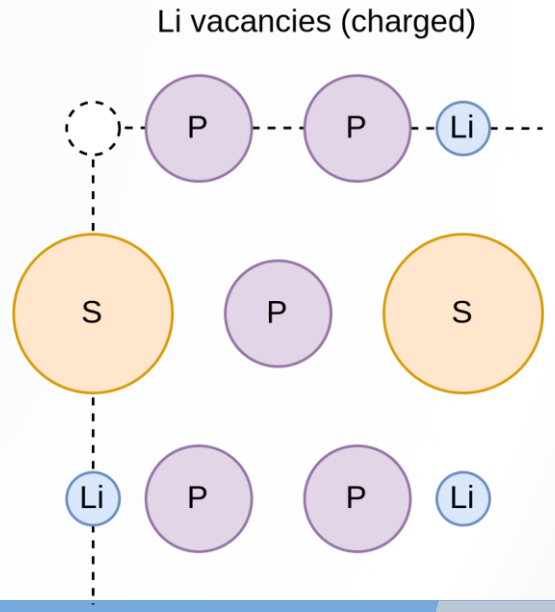

# Model fitting

- Optimizer
  - User-assigned weights for single-objective score
  - Multi-objective algorithms
- Least-squares optimization
  - B-spline coefficients
  - Fit DFT energy, forces, and stresses from atomic configurations
- Fast fitting and fast evaluation allows for LAMMPS-in-the-loop optimization
  - Conservation of energy
  - Diffusion behavior

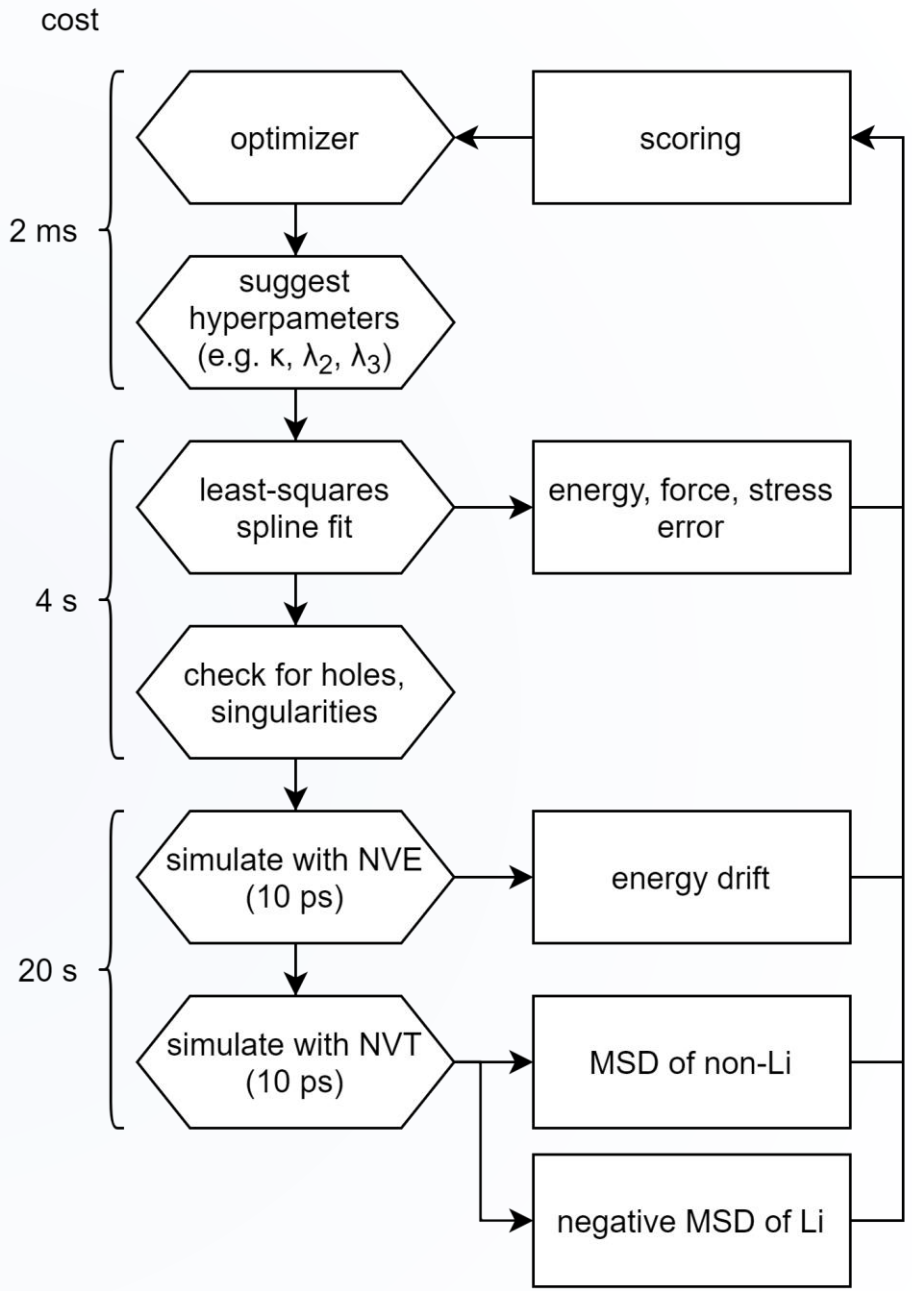

# Computational cost

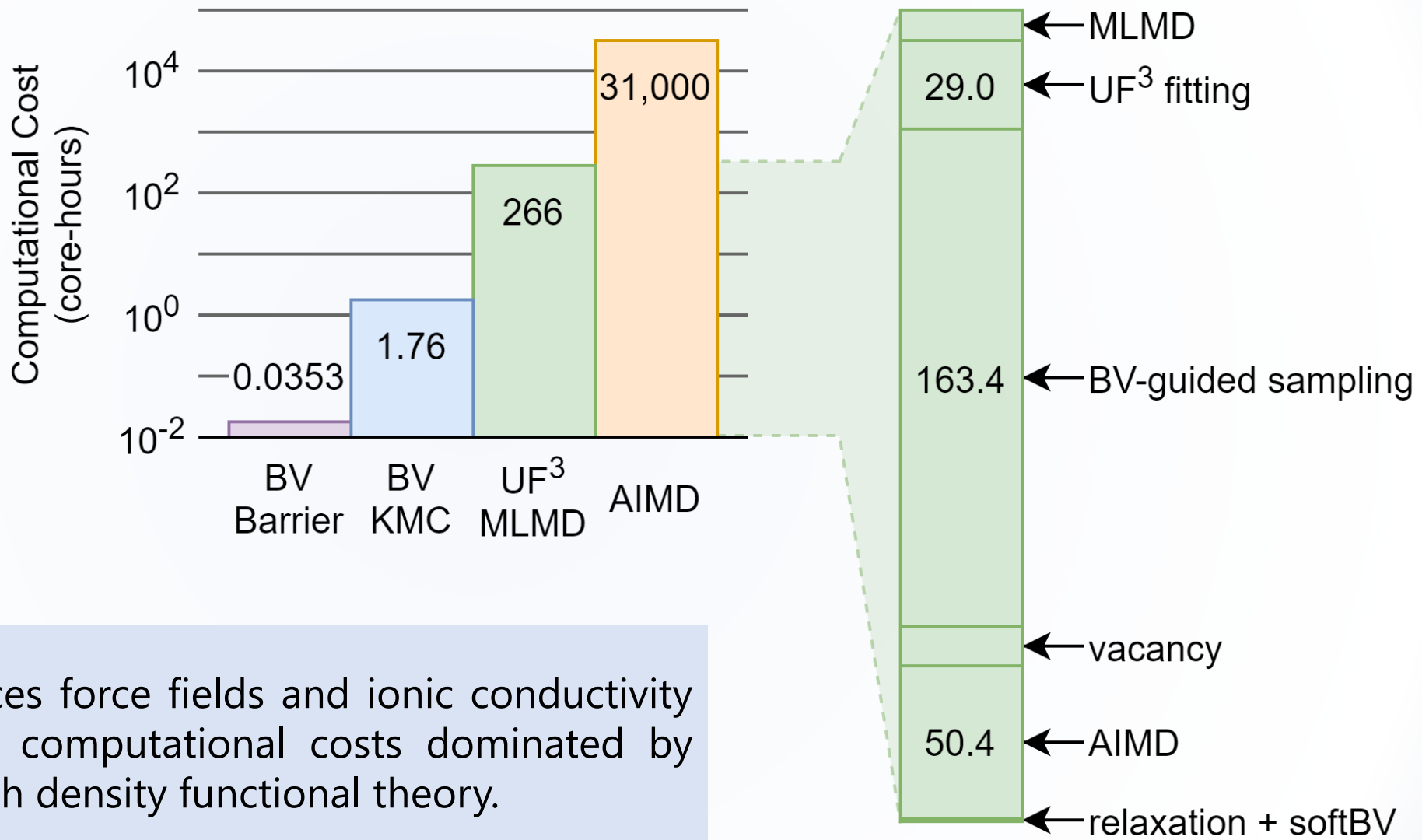


The UF3 framework produces force fields and ionic conductivity predictions with moderate computational costs dominated by generating training data with density functional theory.

# softBV migration barrier as a proxy for ionic conductivity

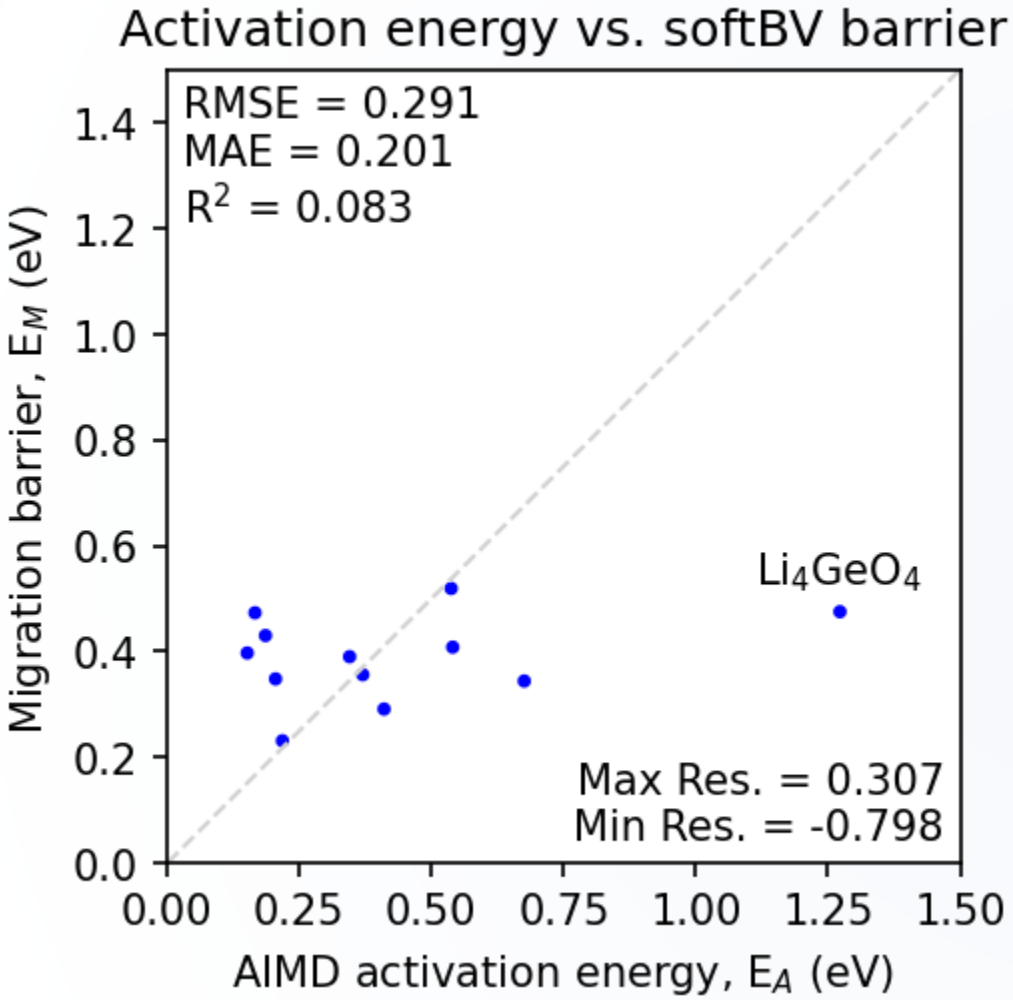


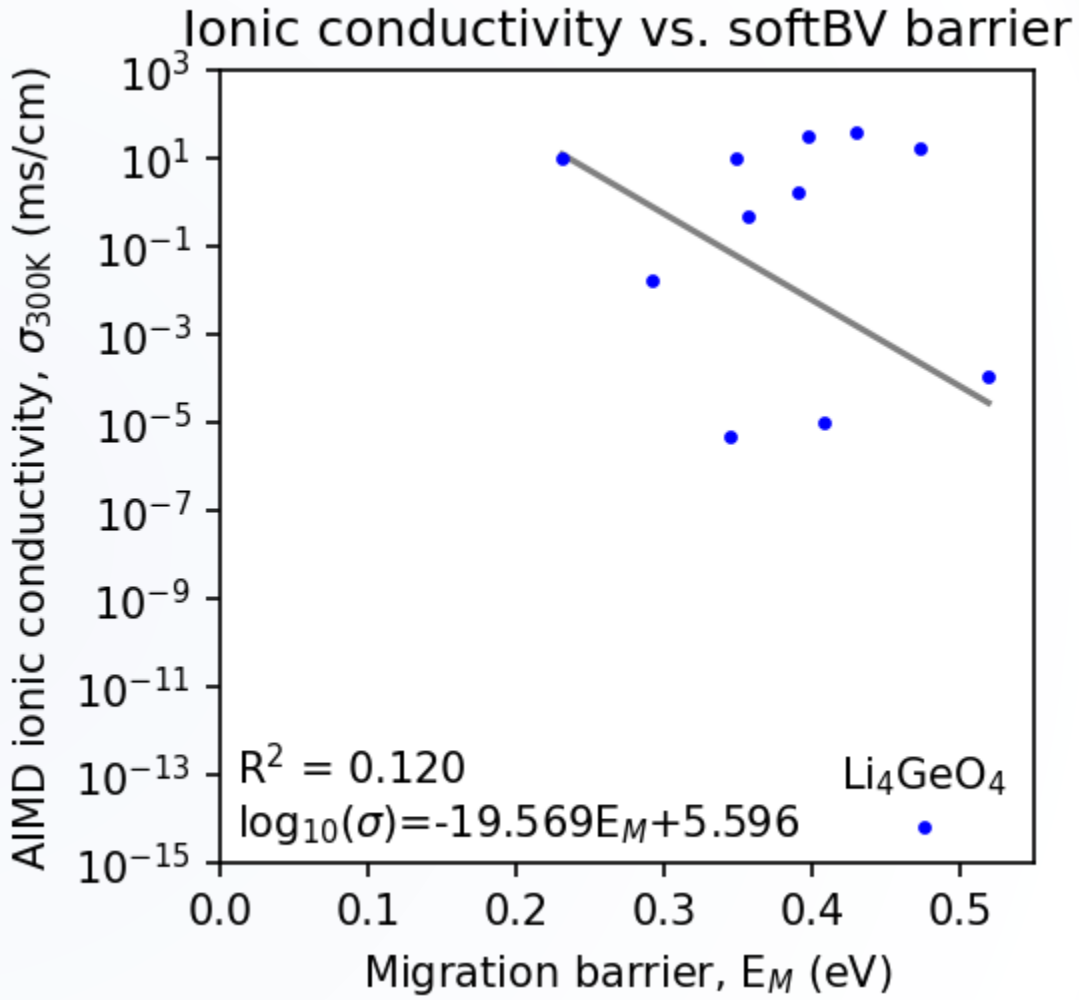


Coarse screening: migration barrier is weakly correlated with both activation energy and ionic conductivity

# Predicting room temperature ionic conductivity

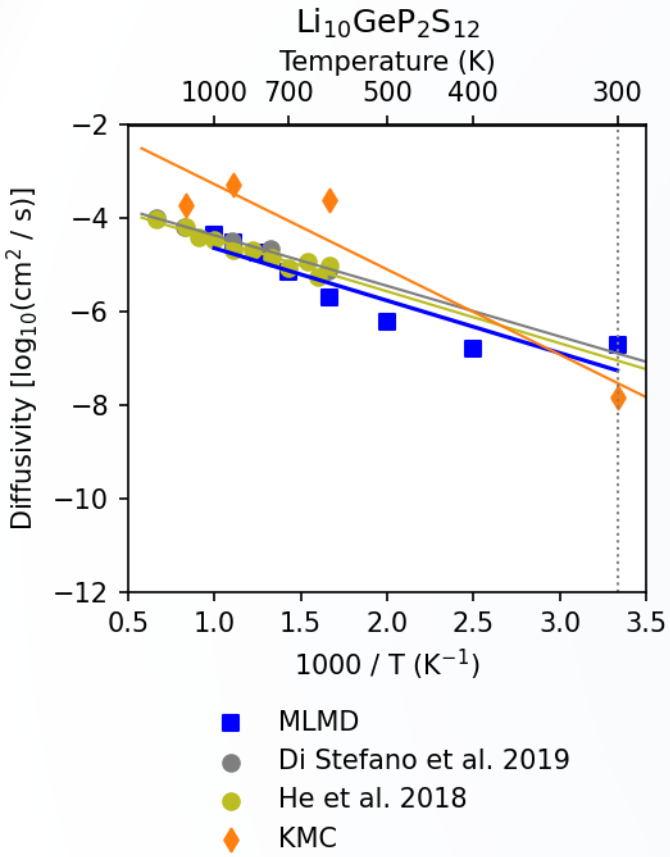


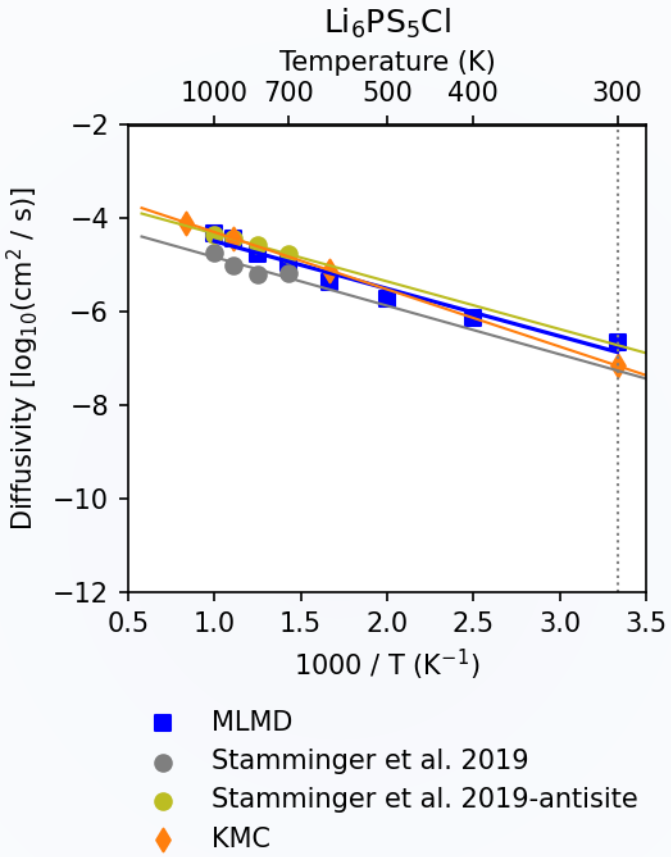


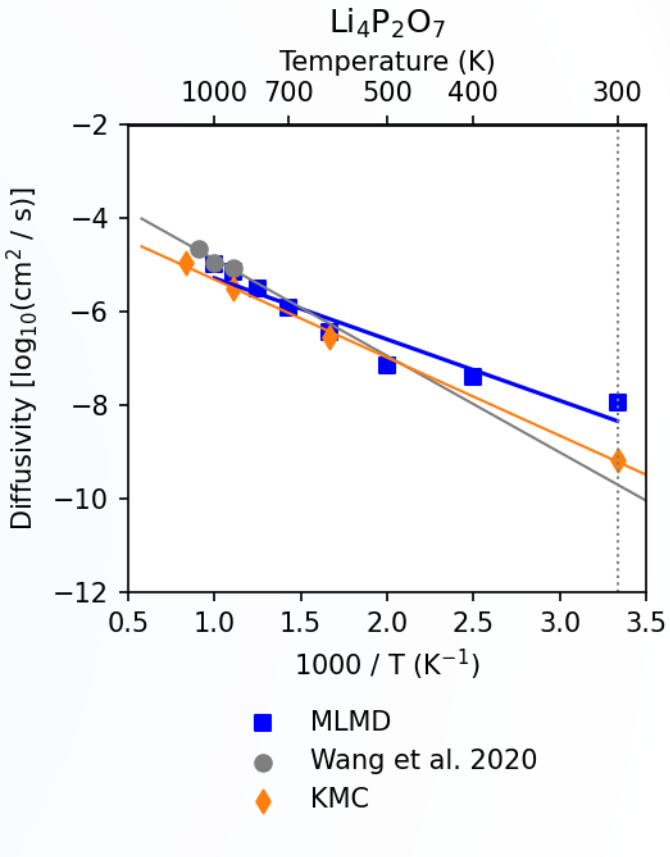


For many materials, both softBV (KMC) and UF3 (MD) yield ionic conductivity predictions in agreement with AIMD.

# Predicting room temperature ionic conductivity

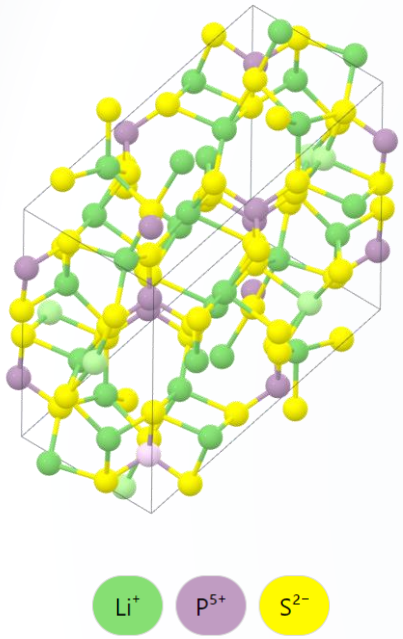


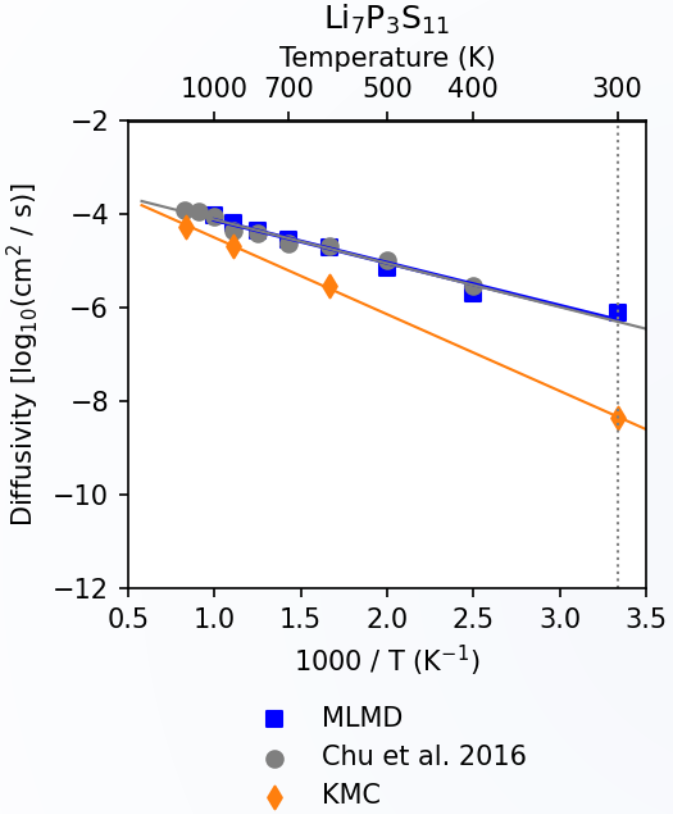


| Formula | Density (0.01 Å$^{-3}$) | Li Density (0.01 Å$^{-3}$) | Spacegroup Number | BV Minima | BV saddle points |
|---|---|---|---|---|---|
| $Li_7P_3S_{11}$ | 5.0 | 1.7 | 2 | **33** | **80** |
| $Li_{10}GeP_2S_1$ | 5.3 | 2.1 | 105 | 15 | 30 |
| $Li_6PS_5Cl$ | 5.0 | 2.3 | 216 | 5 | 7 |
| $Li_6PS_5Br$ | 5.0 | 2.3 | 216 | 5 | 8 |
| $Li_6PS_5I$ | 4.9 | 2.3 | 216 | 5 | 8 |
| $Li_3AlF_6$ | **10.2** | 3.1 | 15 | 16 | 56 |
| $Li_3GaF_6$ | **9.7** | 2.9 | 15 | 16 | 54 |
| $LiZr_2P_3O_{12}$ | 7.2 | **0.4** | 14 | 10 | 25 |
| $LiTi_2P_3O_{12}$ | 8.1 | **0.5** | 167 | **3** | **8** |
| $Li_4P_2O_7$ | 9.1 | 2.8 | 14 | 14 | 42 |
| $Li_2SO_4$ | 8.5 | 2.4 | 14 | 12 | 39 |
| $Li_4GeO_4$ | **10.4** | **4.6** | 63 | 6 | 11 |

Outlier: low symmetry, high number of minima

- High density of nodes in KMC graph
- Shorter hops
- Low MSD → low ionic conductivity

# Predicting room temperature ionic conductivity

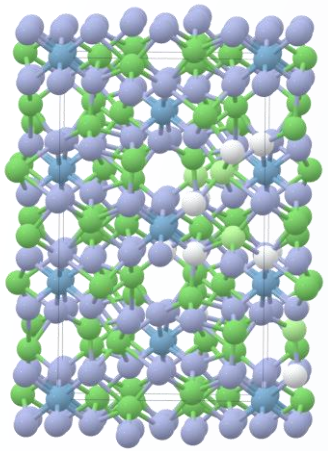


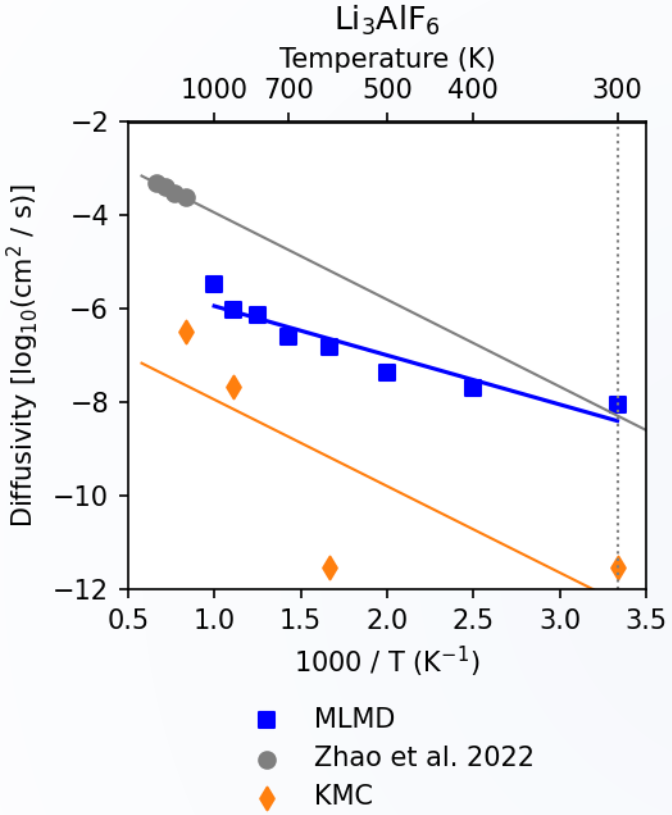


| Formula | Density (0.01 Å$^{-3}$) | Li Density (0.01 Å$^{-3}$) | Spacegroup Number | BV Minima | BV saddle points |
|---|---|---|---|---|---|
| $Li_7P_3S_{11}$ | 5.0 | 1.7 | 2 | **33** | **80** |
| $Li_{10}GeP_2S_1$ | 5.3 | 2.1 | 105 | 15 | 30 |
| $Li_6PS_5Cl$ | 5.0 | 2.3 | 216 | 5 | 7 |
| $Li_6PS_5Br$ | 5.0 | 2.3 | 216 | 5 | 8 |
| $Li_6PS_5I$ | 4.9 | 2.3 | 216 | 5 | 8 |
| $Li_3AlF_6$ | **10.2** | 3.1 | 15 | 16 | 56 |
| $Li_3GaF_6$ | **9.7** | 2.9 | 15 | 16 | 54 |
| $LiZr_2P_3O_{12}$ | 7.2 | **0.4** | 14 | 10 | 25 |
| $LiTi_2P_3O_{12}$ | 8.1 | **0.5** | 167 | **3** | **8** |
| $Li_4P_2O_7$ | 9.1 | 2.8 | 14 | 14 | 42 |
| $Li_2SO_4$ | 8.5 | 2.4 | 14 | 12 | 39 |
| $Li_4GeO_4$ | **10.4** | **4.6** | 63 | 6 | 11 |

Outlier: high number density of atoms

- Dense neighbor lists
- Transferability of softBV parametrization

# Predicting room temperature ionic conductivity

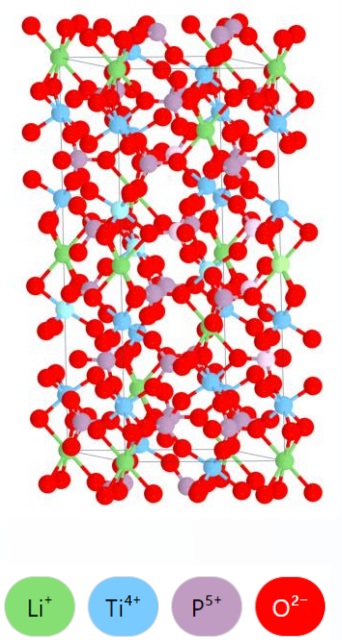


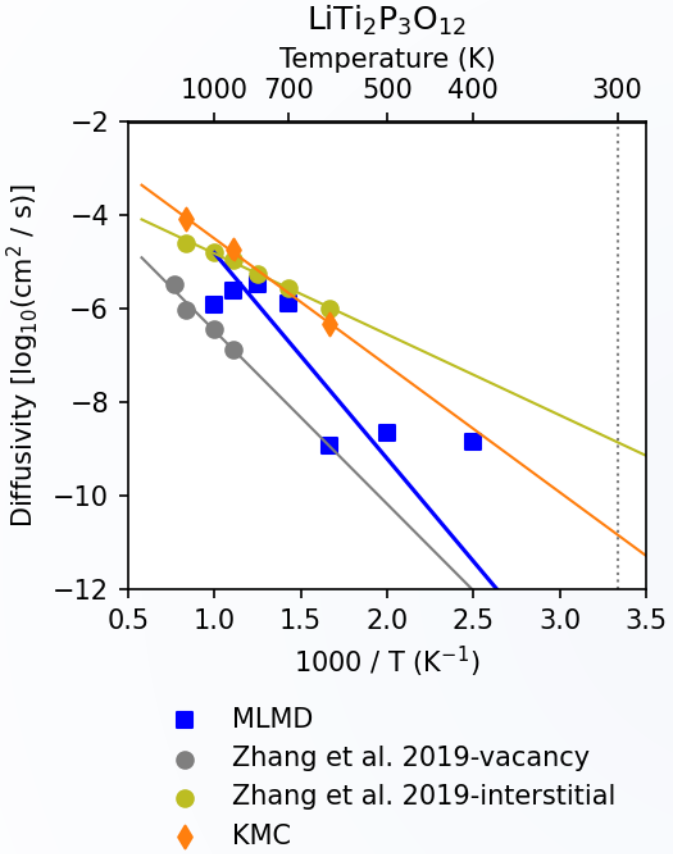


| Formula | Density (0.01 Å$^{-3}$) | Li Density (0.01 Å$^{-3}$) | Spacegroup Number | BV Minima | BV saddle points |
|---|---|---|---|---|---|
| $Li_7P_3S_{11}$ | 5.0 | 1.7 | 2 | **33** | **80** |
| $Li_{10}GeP_2S_1$ | 5.3 | 2.1 | 105 | 15 | 30 |
| $Li_6PS_5Cl$ | 5.0 | 2.3 | 216 | 5 | 7 |
| $Li_6PS_5Br$ | 5.0 | 2.3 | 216 | 5 | 8 |
| $Li_6PS_5I$ | 4.9 | 2.3 | 216 | 5 | 8 |
| $Li_3AlF_6$ | **10.2** | 3.1 | 15 | 16 | 56 |
| $Li_3GaF_6$ | **9.7** | 2.9 | 15 | 16 | 54 |
| $LiZr_2P_3O_{12}$ | 7.2 | **0.4** | 14 | 10 | 25 |
| $LiTi_2P_3O_{12}$ | 8.1 | **0.5** | 167 | **3** | **8** |
| $Li_4P_2O_7$ | 9.1 | 2.8 | 14 | 14 | 42 |
| $Li_2SO_4$ | 8.5 | 2.4 | 14 | 12 | 39 |
| $Li_4GeO_4$ | **10.4** | **4.6** | 63 | 6 | 11 |

Outlier: low Li density, low number of minima and saddle points

- Few nodes for bv-guided sampling means less data for ML
- Transferability of softBV parametrization

# Predicting room temperature ionic conductivity

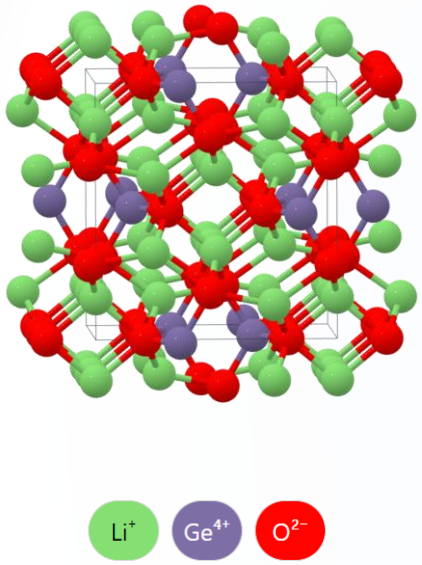


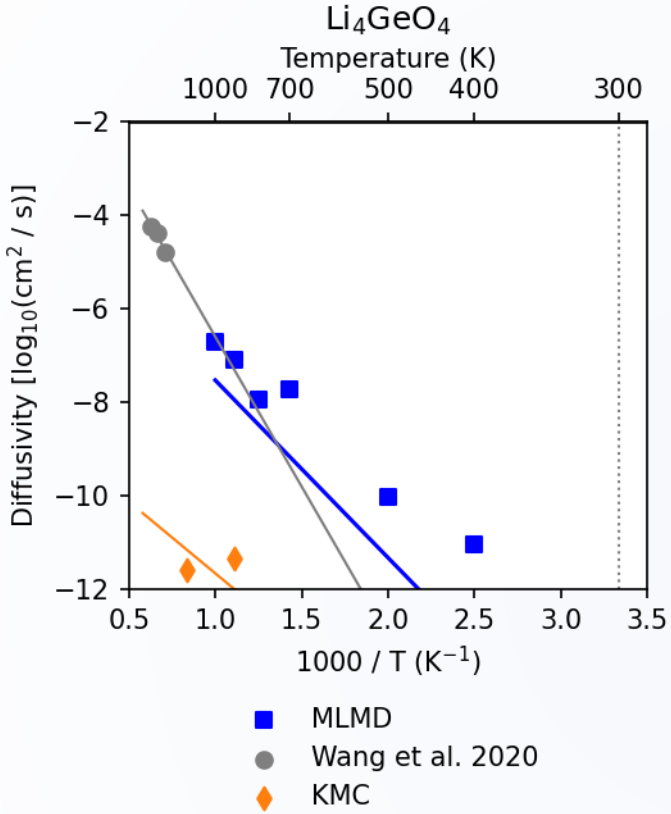


| Formula | Density (0.01 Å$^{-3}$) | Li Density (0.01 Å$^{-3}$) | Spacegroup Number | BV Minima | BV saddle points |
|---|---|---|---|---|---|
| $Li_7P_3S_{11}$ | 5.0 | 1.7 | 2 | **33** | **80** |
| $Li_{10}GeP_2S_1$ | 5.3 | 2.1 | 105 | 15 | 30 |
| $Li_6PS_5Cl$ | 5.0 | 2.3 | 216 | 5 | 7 |
| $Li_6PS_5Br$ | 5.0 | 2.3 | 216 | 5 | 8 |
| $Li_6PS_5I$ | 4.9 | 2.3 | 216 | 5 | 8 |
| $Li_3AlF_6$ | **10.2** | 3.1 | 15 | 16 | 56 |
| $Li_3GaF_6$ | **9.7** | 2.9 | 15 | 16 | 54 |
| $LiZr_2P_3O_{12}$ | 7.2 | **0.4** | 14 | 10 | 25 |
| $LiTi_2P_3O_{12}$ | 8.1 | **0.5** | 167 | **3** | **8** |
| $Li_4P_2O_7$ | 9.1 | 2.8 | 14 | 14 | 42 |
| $Li_2SO_4$ | 8.5 | 2.4 | 14 | 12 | 39 |
| $Li_4GeO_4$ | **10.4** | **4.6** | 63 | 6 | 11 |

Outlier: high number density, low ionic conductivity, high activation energy

- AIMD reference includes few, high temperatures
- Transferability of softBV parametrization

# Predicting activation energy

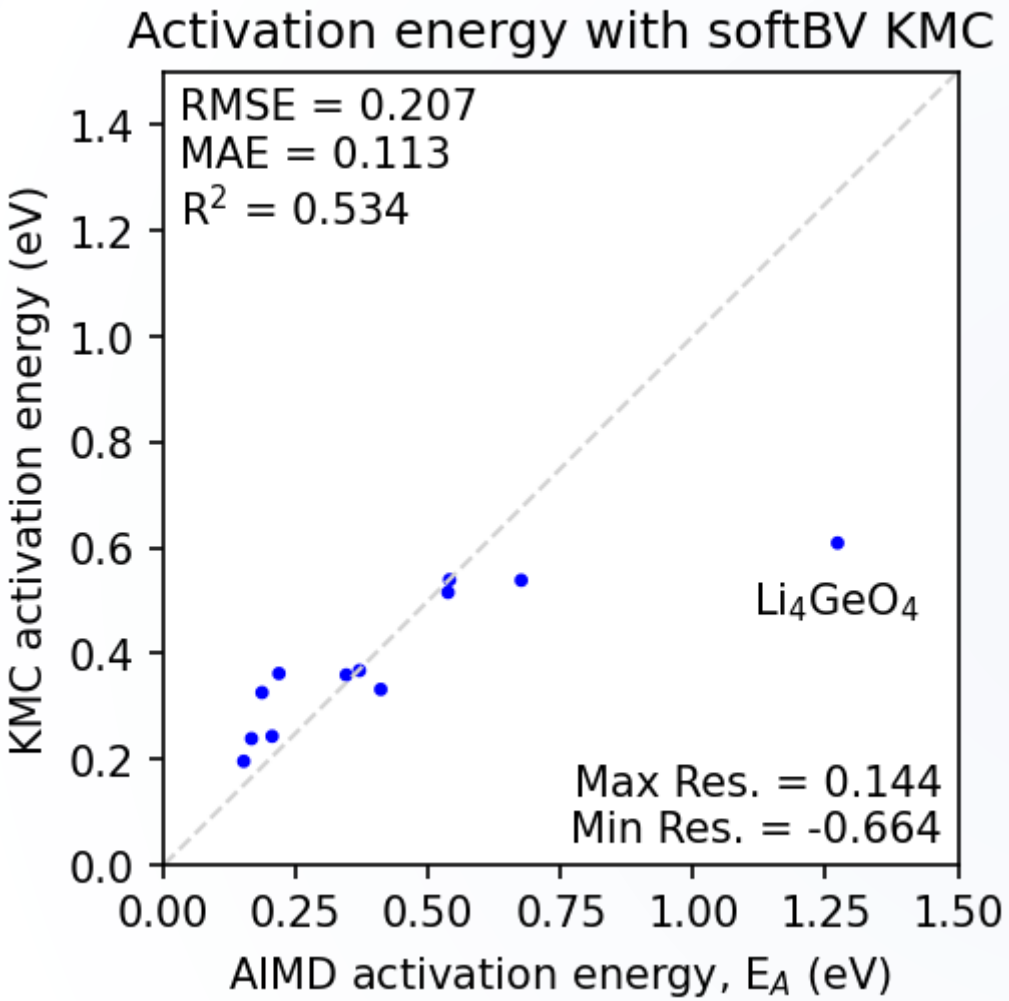


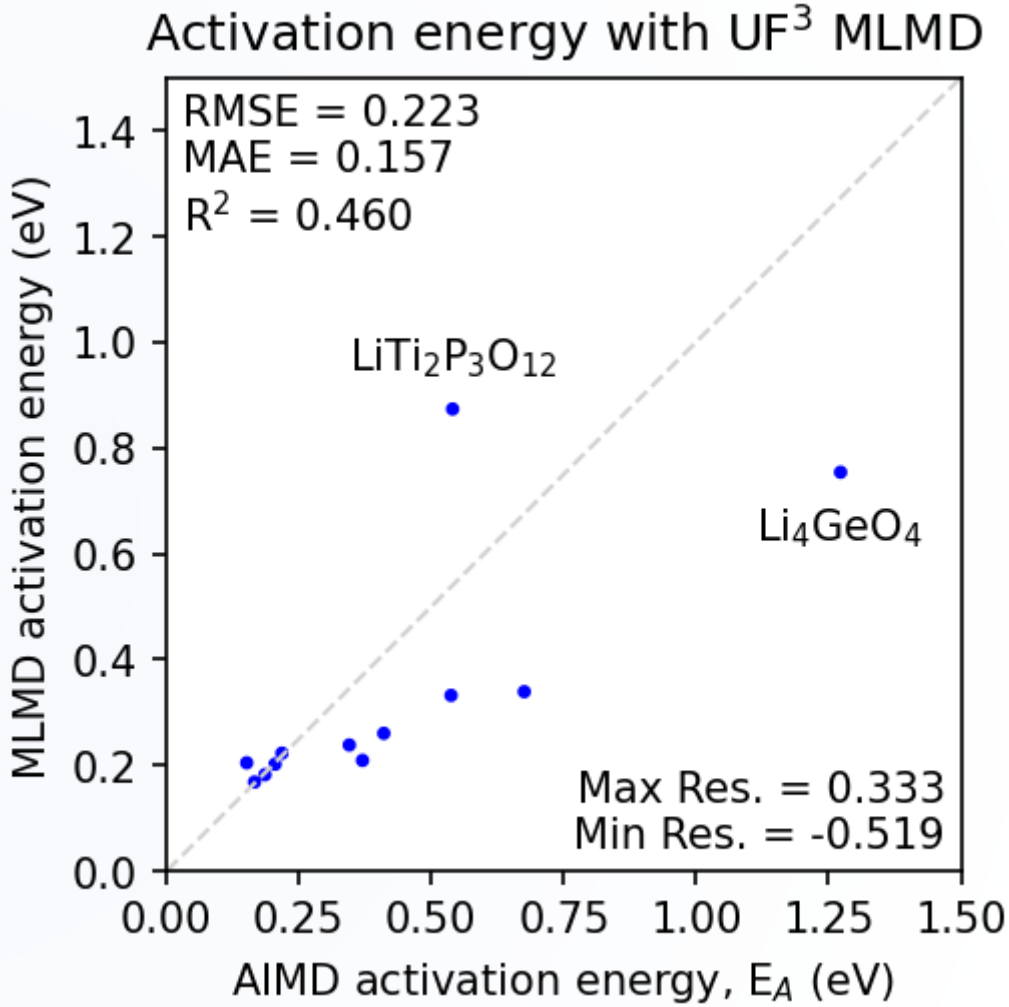


Both methods produce accurate predictions for activation energy

# Predicting room temperature ionic conductivity

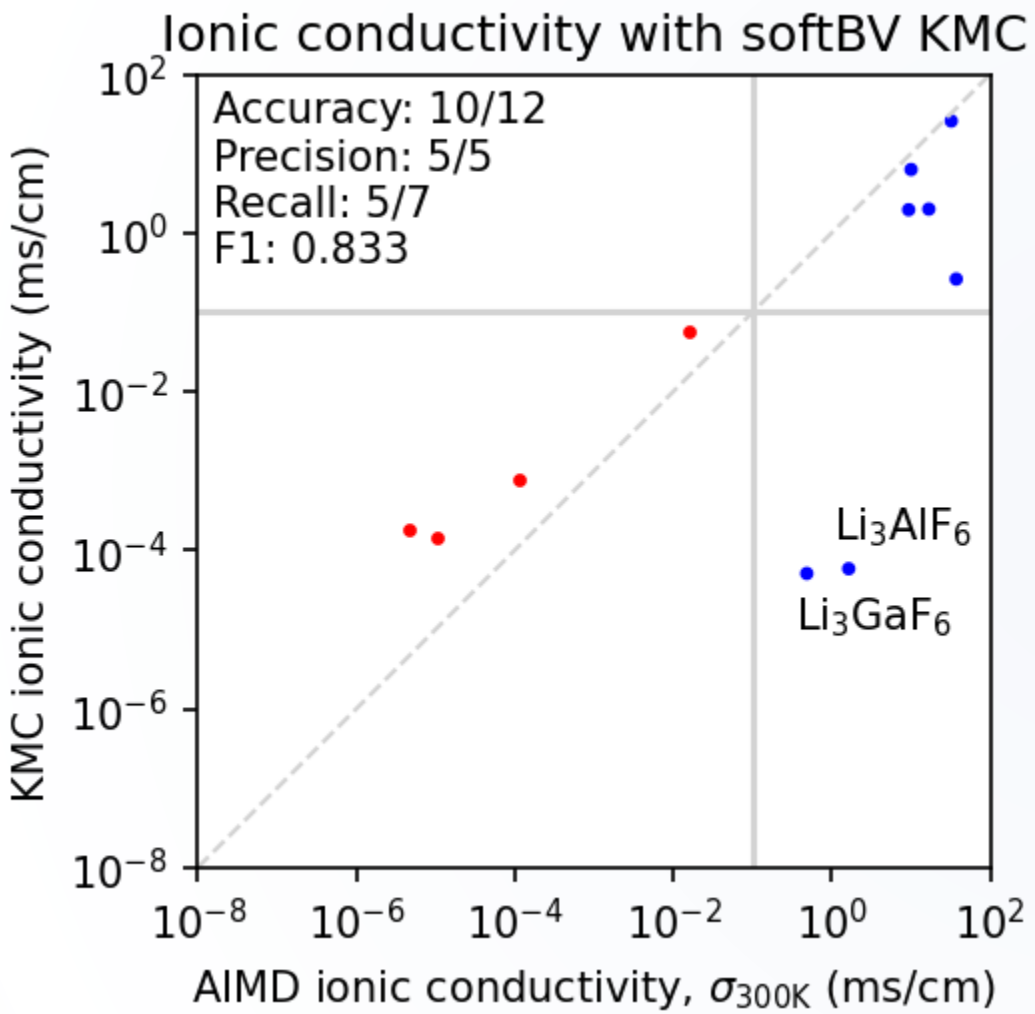


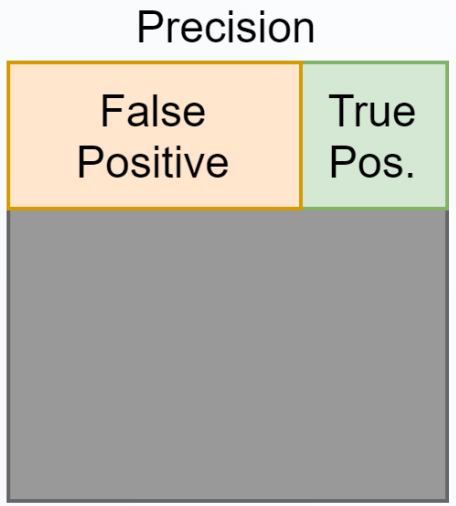


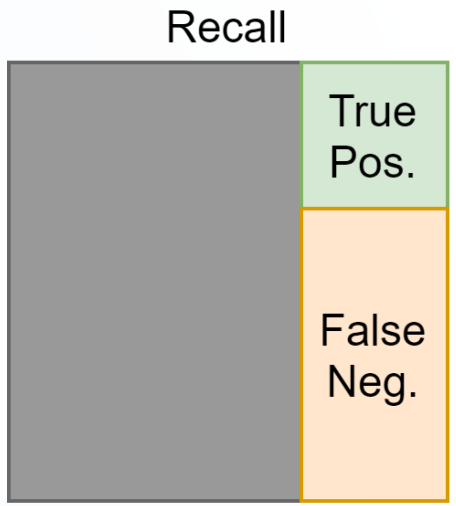


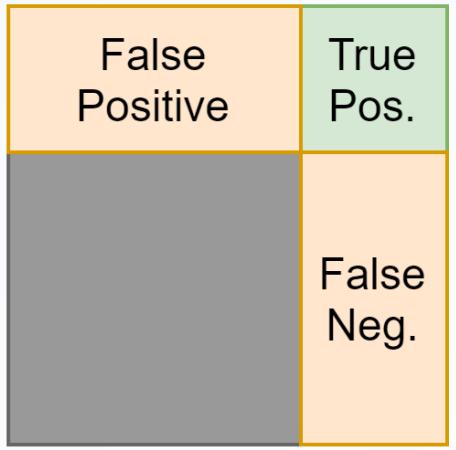


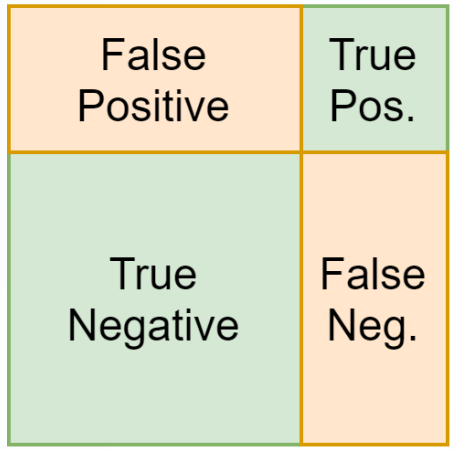

# Predicting room temperature ionic conductivity

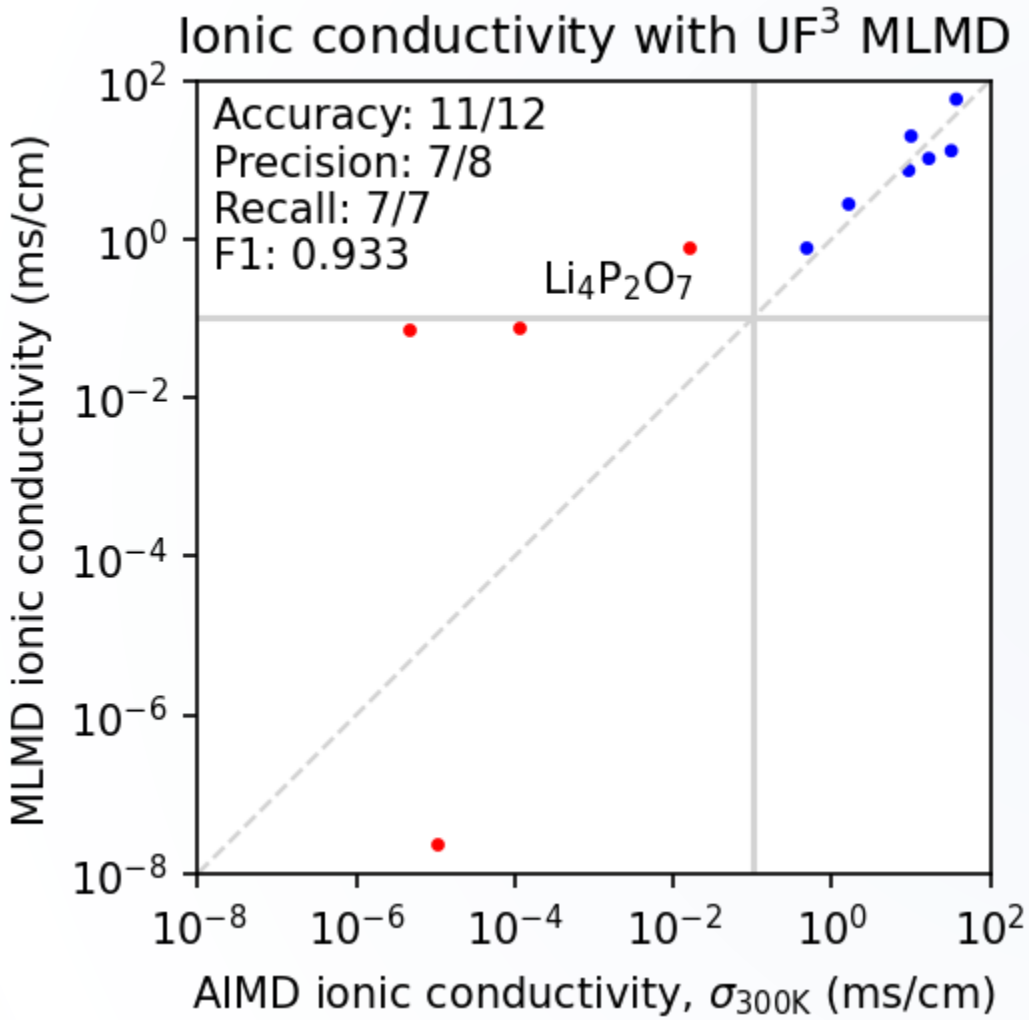


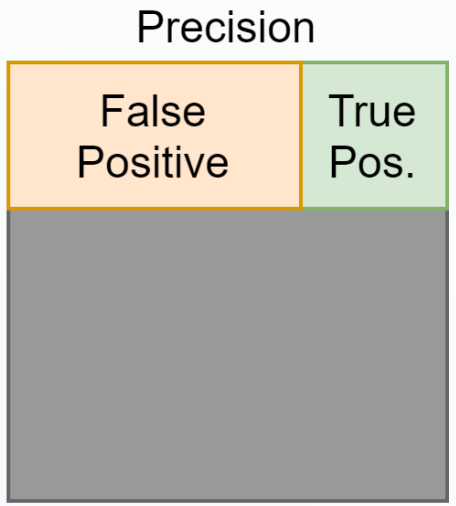


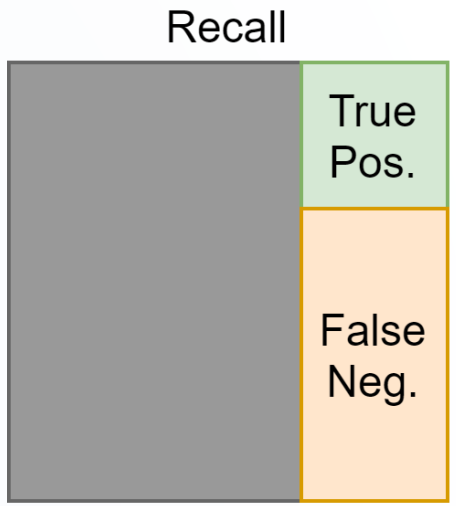


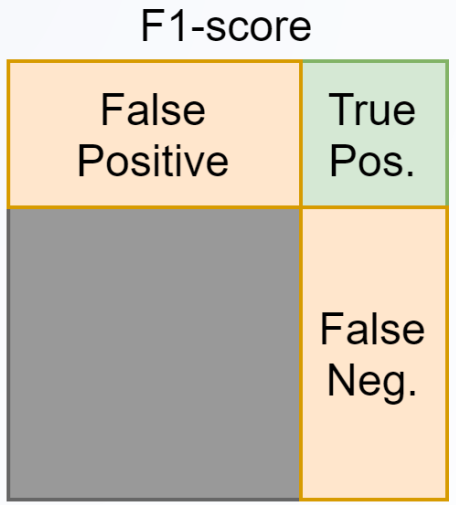


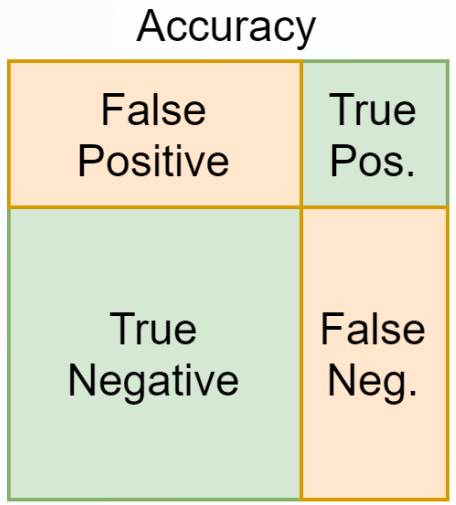

# Hierarchical screening for Li-based solid electrolytes using fast, interpretable machine-learned potentials


Stephen R. Xie, Shreyas J. Honrao, John W. Lawson

Computational Materials Group, NASA Ames Research Center, Moffett Field, CA, USA


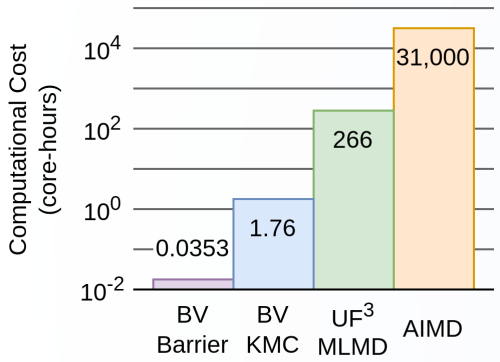


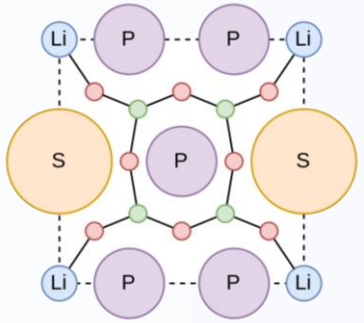


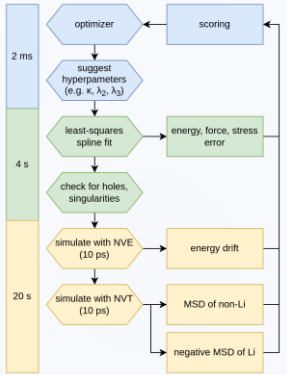


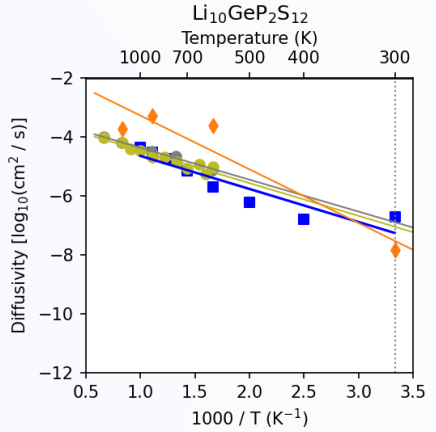


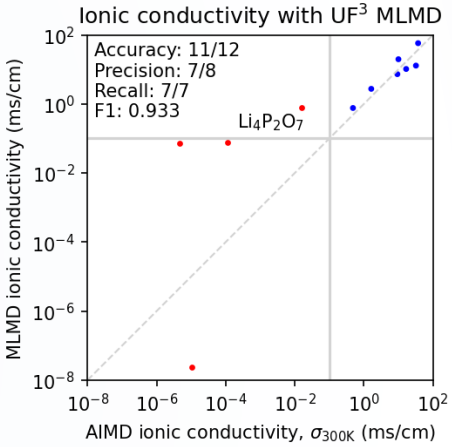


- Pipeline for high-throughput ionic conductivity predictions
- Validating bond valence methods for screening solid-state electrolytes
- Automatic fitting of ultra-fast, interpretable machine-learning force fields